Advances in Nano Research, *Vol. 7 No. 5 (2019) 293-310*
DOI: https://doi.org/10.12989/anr.2019.7.5.293

Thermal buckling analysis of embedded graphene-oxide powder-reinforced nanocomposite plates

Farzad Ebrahimi *[1], Mostafa Nouraei [1], Ali Dabbagh [2] and Timon Rabczuk [3]

[1] *Department of Mechanical Engineering, Faculty of Engineering, Imam Khomeini International University, Qazvin, Iran*
[2] *School of Mechanical Engineering, College of Engineering, University of Tehran, Tehran, Iran*
[3] *Institute of Structural Mechanics (ISM), Bauhaus-University Weimar, Weimar 1599423, Germany*

(*Received December 29, 2018, Revised April 25, 2019, Accepted May 8, 2019*)

Abstract. In this paper, thermal- buckling behavior of the functionally graded (FG) nanocomposite plates reinforced with graphene oxide powder (GOP) is studied under three types of thermal loading once the plate is supposed to be rested on a two-parameter elastic foundation. The effective material properties of the nanocomposite plate are considered to be graded continuously through the thickness according to the Halpin-Tsai micromechanical scheme. Four types of GOPs' distribution namely uniform (U), X, V and O, are considered in a comparative way in order to find out the most efficient model of GOPs' distribution for the purpose of improving the stability limit of the structure. The governing equations of the plate have been derived based on a refined higher-order shear deformation plate theory incorporated with Hamilton's principle and solved analytically via Navier's solution for a simply supported GOP reinforced (GOPR) nanocomposite plate. Some new results are obtained by applying different thermal loadings to the plate according to the GOPs' negative coefficient of thermal expansion and considering both Winkler-type and Pasternak-type foundation models. Besides, detailed parametric studies have been carried out to reveal the influences of the different types of thermal loading, weight fraction of GOP, aspect and length-to-thickness ratios, distribution type, elastic foundation constants and so on, on the critical buckling load of nanocomposite plates. Moreover, the effects of thermal loadings with various types of temperature rise are investigated comparatively according to the graphical results. It is explicitly shown that the buckling behavior of an FG nanocomposite plate is significantly influenced by these effects.

Keywords: thermal buckling; graphene oxide powder; refined higher-order plate theory; elastic foundations

1. Introduction

The possibilities of traditional materials such as metals and their alloys are so exhausted that even when using the most modern techniques it may be difficult to achieve the highest material characteristics and thus higher performance parameters, the durability and reliability of the proposed structures and equipment. Due to this fact, in today's modern world, we can rarely find the industries without utilizing the composite materials due to their distinctive properties that cannot be achieved by any of the constituents alone. The primary reason that composites are chosen for components is because of their remarkable weight saving as well as their relative stiffness and strength. In common, composites are composed of at least two materials, combined to give properties superior to those of the individual constituents. Also, they are typically categorized with respect to their matrix constituent and their reinforcements. Fiber reinforced and laminated composites are the two groups of composites with outstanding properties such as high strength, specific stiffness, high resistance to fatigue failure and large coefficient of thermal expansion which can provide the required engineering properties for the structural purposes. According to the mentioned properties of these groups of composites and their potential to be used in evolving applications, scientists have tried to analyze these materials as more as possible. For example, Kant and Babu (2000) surveyed the thermo-mechanical stability problem of skew fiber reinforced composite (FRC) plates using a shear deformable theorem coupled with the finite element method (FEM). Dynamic behaviors of FRC skew plates are explored by Anlas and Göker (2001) in order to find out the natural frequencies via well-known Ritz method. In other researches, a combination of both analytical and experimental investigation is utilized to study the buckling behavior of both cantilever I and open channel beams by considering shear effects (Qiao *et al*. 2003, Shan and Qiao 2005). Also, for the laminated composites (LCs), Liu *et al*. (2002) presented an investigation on the buckling analysis of isotropic and symmetrically LC plates via an element-free Galerkin method to show the efficiency of this method. Afterwards, the first-order shear deformation theory was employed by Shan and Qiao (2005) in order to analyze the free vibration of a kind of laminated composites which is thick and symmetrical. A global-local higher-order theory was presented by Zhen and Wanji (2006) to probe the free vibration problem of LC plates. Urthaler and Reddy (2008) investigated the bending response of LC plates to find out an accurate prediction of the global bending response of

*Corresponding author, Ph.D., Professor,
E-mail: febrahimy@eng.ikiu.ac.ir

Copyright © 2019 Techno-Press, Ltd.

ISSN: 2287-237X (Print), 2287-2388 (Online)

thin and moderately thick plates subjected to large rotation. They considered for the nonlinearity effects within the framework of von-Karman strain-displacement relations. Shariyat (2010) introduced a new theory for analyzing the thermally affected mechanical characteristics of sandwich plates to cover the continuity conditions between layers. The effects of nonlinear elastic substrate on the static stability responses of the LC plates are considered by Baltacıoğlu *et al*. (2011) using a first-order shear deformation theory coupled with the nonlinear relations of von-Karman. Also, some investigations have been performed on LCs via non-uniform rational B-splines (NURBS) method (Shojaee *et al*. 2012, Thai *et al*. 2012). Carrera Unified Formulation (CUF) was employed by Tornabene *et al*. (2014) in order to analyze the stability problem of doubly-curved shells. The Fourier-Ritz method was applied by Wang *et al*. (2017) with the aim of analyzing the vibrational behavior of LC shells and panels by considering various boundary conditions (BCs). Also some mechanical analysis of the FG sandwich plates have been investigated by the Menasria *et al*. (2017) based on the analytical approaches. Sobhani *et al*. (2018) solved the stability problem of LC with respect to the delamination effects in the framework of acoustic emission and signal processing techniques.

Micro and nanostructures have been introduced as novel materials whose size of elemental structure has been engineered at the micro or nanometer scale. The curiosity of the researchers has been driven into nanostructures due to the novel applications of these structures in almost all branches of technology. For instant, the dynamic and static behaviors of some microstructures have been analyzed recently to show hoe these structures can be applicable for engineering purposes. Some mechanical responses of the nanobeams such as have been investigated by Bellifa et al. (2017) on the basis of nonlocal shear deformation theory. Several effects such as thermal loadings, elastic foundations and magnetic field are applied to the nanostructures like nanobeams and nanoplates by the researchers (Karami *et al*. 2017) in order to find out how these effects can influence the buckling and vibrational responses of these nanostructures. The wave propagation analysis of the nanoshells and magneto-electro-elastic (MEE) nanotubes have been investigated by Ebrahimi *et al*. (2019) based on the nonlocal strain gradient elasticity theory. In addition, the wave dispersion analysis of the rotating FG nanobeams have been conducted by the same authors (Ebrahimi *et al*. 2018a, Ebrahimi and Haghi 2018b) by utilizing nonlocal elasticity theory. Moreover, considering the thermal effect on the wave propagation analysis of the rotation nanostructures for different purposes have been carried out by the same authors (Ebrahimi and Haghi 2018a, Ebrahimi *et al*. 2018b). Some of researchers in recent years have analyzed mechanical behaviors of FGM nanoplates based on various plate shear deformation plate theories. (Ebrahimi and Barati 2016a-e, Ebrahimi *et al*. 2016, Ebrahimi and Dabbagh 2016, Ebrahimi and Hosseini 2016a, b). Analysis of nano-structure's mechanical behaviors is one of recent interesting research topics. (Ebrahimi and Barati 2016f-n, 2017).

Most recently, Arefi *et al*. (2019) have studied the bending responses of the curved nanobeams which are reinforced with the GPLs and embedded on Pasternak foundation based on the first-order shear deformation theory. Also, the buckling analysis of the FG magneto-electro-elastic nanoplates have been conducted by Ebrahimi and Barati (2019) with employing the Eringen's nonlocal elasticity theory.

Furthermore, once elements with at least one dimension in nano scale are selected as reinforcements, the composite is named a nanocomposite. Indeed, the outstanding mechanical properties of nanoparticles were appealing enough in the engineers' opinion to be employed as reinforcement in composites. One of the most famous nano size reinforcing elements is carbon nanotube (CNT) which is an important new class of technological materials that possesses numerous novel and useful properties. Therefore, it is of high importance to analyze the mechanical behaviors of CNT reinforced (CNTR) nanocomposites. In a remarkable endeavor, the Eshelby-Mori-Tanaka homogenization model was employed by Formica *et al*. (2010) to investigate the vibration behavior of CNTR nanocomposites via FEM. Single-walled CNTs (SWCNTs) have attracted the attention of the researchers recently with their evolving applications such as reinforcements in composites, additives in polymers, catalysts and so on. For example, Shen and Zhang (2010) investigated both thermo-elastic pre- and post-buckling response of nanocomposite plates reinforced with SWCNTs to show how the nanofillers' distribution type can improve the stability limits of nanocomposite plates. Also, Arani *et al*. (2011) employed both FE and analytical methods to investigate effects of some variants such as aspect ratio, BCs and CNTs' orientation on the buckling loads of SWCNT reinforced LC plates. Wang and Shen (2011) presented a thermal analysis on the nonlinear vibrational behaviors of nanocomposite plates reinforced with SWCNTs via a higher-order plate theory. Both static and dynamic FEM analyses of SWCNT reinforced nanocomposite plates have been performed by Zhu *et al*. (2012) by considering different types of reinforcements' distributions. In addition, Shen and Xiang (2012) probed the nonlinear thermal vibration behaviors of CNTR nanocomposite shells with respect to various distribution patterns of nanofillers. Yas and Samadi (2012) solved the vibration and buckling problems of the CNTR nanocomposite beams numerically by considering the influences of elastic foundation. Moreover, Wattanasakulpong and Ungbhakorn (2013) surveyed bending, buckling and vibration behaviors of the embedded nanocomposite beams reinforced with SWCNTs by the means of Navier method. Lei *et al*. (2013) implemented the Eshelby-Mori-Tanaka homogenization technique to account for the nanotubes' aggregation while investigating the buckling behaviors of CNTR nanocomposite plates via a FE based element-free method. In another research, Liew *et al*. (2014) introduced a meshless approach for the purpose of studying the post-buckling responses of axially compressed CNTR nanocomposite panels. Also, Zhang *et al*. (2015) employed first-order shear deformation plate theory incorporated with Ritz method to analyze the vibrational

behaviors of CNTR skew nanocomposites. Wu *et al*. (2016) found it significant to account for the geometrical imperfections once examining the nonlinear vibration behaviors of FG-CNTR nanocomposite beams. Ebrahimi and Farazmandnia (2017) employed a higher-order shear deformation beam theory to analyze the thermo-mechanical vibration of sandwich beams with FG-CNTR nanocomposite face sheets. Ebrahimi and Rostami (2018) have just analyzed the wave propagation problem of CNTR nanocomposite beams via different shear deformation theories. Also, Bakhadda *et al*. (2018) carried out the dynamic and bending analyses of the CNTR nanocomposites. Most recently, SafarPour *et al*. (2019) have carried out an analysis on the free vibration and buckling behaviors of piezoelectric rotating cylindrical CNTR nanocomposite shells with the aim of investigating the effect of applying critical voltage on the structure. Moreover, Mehar *et al*. (2019) and Torabi *et al*. (2019) implemented the numerical methods in order to find out the buckling responses of the CNTR nanocomposite shells and plates in thermal environments.

On the other hand, CNTs are not the only nano size reinforcement which is used in the nanocomposites. Nano fillers consisted of other carbon based materials are utilized in nanocomposites, too. For instant, graphene platelets (GPLs) and graphene oxide powders (GOPs) are recently employed by researchers to design and analyze novel nanocomposites. Suk *et al*. (2010) investigated the mechanical properties of the GO by combining the AFM measurement with the FEM in a new approach for evaluating the mechanical properties of ultrathin membranes. The static stability analysis of the single layer graphene sheets with focus on buckling behavior of this material, have been conducted by Bouadi *et al*. (2018) by utilizing new shear deformation theory. The Halpin-Tsai model was employed by Feng *et al*. (2017) for homogenization of the nanocomposites in order to investigate the effects of using GPLs, as reinforcements in a nanocomposite, on the nonlinear bending responses of a beam. Also, a higher-order plate model is incorporated with the nonlinear theory of von-Kármán by some of the authors in order to consider for the impacts of thermal environment and elastic medium on the nonlinear bending and vibration characteristics of functionally graded graphene-reinforced composite (FG-GRC) laminated plates (Shen *et al*. 2017a, b). Also, the issue of postbuckling problem of a porous GPL reinforced (GPLR) nanocomposite beam is undertaken and studied by Barati and Zenkour (2017) with respect to the influences of geometrical imperfection. Yang *et al*. (2017) carried out an analysis on the stability of FG nanocomposite beams reinforced with GPLs. Also, Zhao *et al*. (2017) studied the bending and vibration behaviors of an FG trapezoidal plate reinforced with GPLs by employing the modified Halpin-Tsai model and the rule of mixture to predict the effective material properties. Besides, researchers have also probed the vibration, bending and compressive buckling of the GPLR polymeric nanocomposite plates via Mindlin-Reissner theory (Song *et al*. 2018). Most recently, Qaderi *et al*. (2019) carried out an investigation on the vibration behavior of the GPLR nanocomposite beams rested on viscoelastic foundation. Also, Thai *et al*. (2019) investigated the dynamic and static responses of the GPLR polymeric nanocomposite plates by considering uniform and non-uniform distribution patterns of GPL based on the NURBS formulation. In addition, the effects of thermal loadings and external pressure on the buckling behavior of the graphene sheets reinforced shells investigated by Kiani (2019) based on the first-order shear deformation theory.

Graphene oxide also is a novel nanofiller with astounding thermal (Balandin *et al*. 2008, Cai *et al*. 2010), mechanical and optical properties (Yazid *et al*. 2018). In the recent years, it is found that graphene oxide can be a great reinforcement for the plates with polymer matrix in order to enhance the mechanical and functional properties of the polymer materials due to its remarkable compatibility with polymers (Potts *et al*. 2011). The experiments on this novel nanofiller show that monolayer GO has the Young modulus of 0.25 ± 0.15 TPa (Gómez-Navarro *et al*. 2008). Due to this fact, nanocomposites reinforced with GO have extraordinary tensile strength in addition to their low cost. GO has been also used in fabricating flexible displays and transparent conducting films, accumulators, and supercapacitors (Mikoushkin *et al*. 2011). Moreover, owing to the GOs' hierarchical structure, it can be utilized as an adsorbent material. Recently, Zhang *et al*. (2018) surveyed the buckling, bending and vibration of the GOP reinforced (GOPR) nanocomposite beams via Timoshenko theory. Except the aforementioned paper, no other research can be found dealing with the mechanical behaviors of nanocomposite continuous systems reinforced with GOPs. To the authors' best knowledge, the thermal buckling problem of an embedded FG-GOPR nanocomposite plate, subjected to different types of temperature rise, has never been studied up to now.

Present research is devoted to include the effects of foundations' stiffness and distribution patterns of nanofillers on the thermal-buckling responses of a FG nanocomposite plate reinforced with GOPs once the plate is subjected to temperature gradient. The material properties are achieved from Halpin-Tsai micromechanical scheme. Moreover, a refined higher-order plate model is mixed with the Hamilton's principle to reach the governing equations. Afterwards, Navier's method is implemented to solve the eigenvalue problem and compute the critical buckling load for a simply-supported plate. Also, three types of thermal loading are taken into account. Finally, the influences of different variants are illustrated via non-dimensional form of the parameters are presented for the sake of simplicity.

2. Theory and formulation

2.1 Material homogenization

The studied structure is consisted of an initial polymer matrix that is strengthened via a group of GOPs. The reinforcements are dispersed in the primary material via different patterns. These patterns can be generated by putting the nanofillers in a series of specified positions

which can be calculated by following simple modeling

$$\begin{cases} V_{GOP} = V_{GOP}^{*}\text{GOPR-U} \\ V_{GOP} = \left(2 - 4\dfrac{|z|}{h}\right) V_{GOP}^{*}\text{GOPR-O} \\ V_{GOP} = 4\dfrac{|z|}{h} V_{GOP}^{*}\text{GOPR-X} \\ V_{GOP} = (1 + 2\dfrac{z}{h}) V_{GOP}^{*}\ \text{GOPR-V} \end{cases} \tag{1}$$

in which V_{GOP}^{*} stands for the total volume fraction of GOPs and can be formulated as

$$V_{GOP}^{*} = \frac{W_{GOP}}{W_{GOP} + \left(\frac{\rho_{GOP}}{\rho_M}\right)(1 - W_{GOP})} \tag{2}$$

where *GOP* and *M* subscripts are related to GOP reinforcements and the matrix, respectively. In addition, ρ stands for mass density and W_{GOP} denotes GOP weight fraction. Afterwards, it is necessary to earn the effective Young's modulus and the effective Poisson's ratio of the nanocomposite. Herein, the Halpin-Tsai homogenization technique is extended for derivation of the material properties (Van Es 2001, Zhang *et al*. 2018). Now, the Young's modulus can be written as

$$E_{eff} = 0.49E_l + 0.51E_t \tag{3}$$

where E_l and E_t account for longitudinal and transverse Young's modulus of the composite, respectively. These elastic parameters can be calculated as (Zhang *et al*. 2018)

$$E_l = \frac{1 + \xi_l \eta_l V_{GOP}}{1 - \eta_l V_{GOP}} \times E_M, \qquad E_t = \frac{1 + \xi_t \eta_t V_{GOP}}{1 - \eta_t V_{GOP}} \times E_M \tag{4}$$

Where

$$\eta_l = \frac{\left(\frac{E_{GOP}}{E_M}\right) - 1}{\left(\frac{E_{GOP}}{E_M}\right) + \xi_l}, \quad \eta_t = \frac{\left(\frac{E_{GOP}}{E_M}\right) - 1}{\left(\frac{E_{GOP}}{E_M}\right) + \xi_t} \tag{5}$$

in which E_{GOP} and E_M stand for GOPs and matrix Young modulus, respectively. Also, the geometry factors (ξ_l, ξ_t) can be computed in the following form (Zhang *et al*. 2018)

$$\xi_l = \xi_t = \frac{2d_{GOP}}{h_{GOP}} \tag{6}$$

in which d_{GOP} and h_{GOP} are related to diameter and thickness of GOPs, respectively. Now, the effective Poisson's ratio of the composite can be achieved by using the rule of mixture in the following form

$$\nu_{eff} = \nu_{GOP} V_{GOP} + \nu_M V_M \tag{7}$$

where V_{GOP} and V_M correspond with the volume fractions of GOPs and matrix, respectively. It is worth mentioning that the effective mass density can be computed in the same form as Poisson's ratio is achieved in Eq. (7). The volume fractions are related to each other as

$$V_{GOP} + V_M = 1 \tag{8}$$

Now, it is turn to calculate the coefficient of thermal expansion (CTE) for the GOPR nanocomposite in the following form Van Es (2001)

$$\alpha_{eff} = \alpha_M + \frac{\alpha_M + \alpha_{GOP}}{\frac{1}{K_M} + \frac{1}{K_{GOP}}}\left[\frac{1}{K_{eff}} + \frac{1}{K_M}\right] \tag{9}$$

in which *K* is the bulk moduli and α is the CTE. Also, the M and GOP subscript is referred to the matrix and graphene oxide powder respectively.

2.2 Refined higher-order plate theory

The classical theory of plates possesses some simplifying assumptions which leads to some limitations in modeling. For example, this theory cannot present reliable results whenever the length-to-thickness ratio is inside 10. Due to this fact, the researchers have introduced some mathematical modeling which is able to estimate the shear stress and strain of the plates and beams (Abdelaziz *et al*. 2017). Moreover, Bourada *et al*. (2019) employed sinusoidal shear deformation theory in order to investigate the dynamic behavior of the FG porous beam. In comparison to the other works in which the thickness stretching effect is taken into account (Bouhadra *et al*. 2018) the very small difference was seen on the vibration and stability analysis of FG plates which could be negligible for the sake of simplicity. On the other hand, in some other researches, other versions of the classical kinematic theories are presented which are modified to be applicable in the cases that influences of the shear deformation cannot be ignored. For the purpose of capturing the shear effect in the higher-order theorems, a shape function is presented in each theory. In this paper, the refined form of sinusoidal plate theory is utilized in order to achieve the kinematic relations of the plate. According to this theory, the displacement field of a plate can be written as

$$u_x(x,y,z) = u(x,y) - z\frac{\partial w_b}{\partial x} - f(z)\frac{\partial w_s}{\partial x} \tag{10}$$

$$u_y(x,y,z) = v(x,y) - z\frac{\partial w_b}{\partial y} - f(z)\frac{\partial w_s}{\partial y} \tag{11}$$

$$u_z(x,y,z) = w_b(x,y) + w_s(x,y) \tag{12}$$

where, *u* is longitudinal displacement and w_b, w_s are bending and shear deflections, respectively. The corresponding shape function of the employed theory can be expressed as

$$f(z) = z - \frac{h}{\pi} sin\left(\frac{\pi z}{h}\right) \tag{13}$$

The nonzero strains of the plate can be expressed by following equations

$$\begin{Bmatrix}\varepsilon_x\\ \varepsilon_y\\ \gamma_{xy}\end{Bmatrix}=\begin{Bmatrix}\varepsilon_x^0\\ \varepsilon_y^0\\ \gamma_{xy}^0\end{Bmatrix}+z\begin{Bmatrix}k_x^b\\ k_y^b\\ k_{xy}^b\end{Bmatrix}+f(z)\begin{Bmatrix}k_x^s\\ k_y^s\\ k_{xy}^s\end{Bmatrix},\quad \begin{Bmatrix}\gamma_{yz}\\ \gamma_{xz}\end{Bmatrix}=g\begin{Bmatrix}\gamma_{yz}^s\\ \gamma_{xz}^s\end{Bmatrix} \tag{14}$$

where

$$\begin{Bmatrix}\varepsilon_x^0\\ \varepsilon_y^0\\ \gamma_{xy}^0\end{Bmatrix}=\begin{Bmatrix}\dfrac{\partial u}{\partial x}\\ \dfrac{\partial v}{\partial y}\\ \dfrac{\partial u}{\partial y}+\dfrac{\partial v}{\partial x}\end{Bmatrix},\quad \begin{Bmatrix}k_x^b\\ k_y^b\\ k_{xy}^b\end{Bmatrix}=\begin{Bmatrix}\dfrac{-\partial^2 w_b}{\partial x^2}\\ \dfrac{-\partial^2 w_b}{\partial y^2}\\ -2\dfrac{\partial^2 w_b}{\partial x\partial y}\end{Bmatrix},$$
$$\begin{Bmatrix}k_x^s\\ k_y^s\\ k_{xy}^s\end{Bmatrix}=\begin{Bmatrix}\dfrac{-\partial^2 w_s}{\partial x^2}\\ \dfrac{-\partial^2 w_s}{\partial y^2}\\ -2\dfrac{\partial^2 w_s}{\partial x\partial y}\end{Bmatrix}\quad \begin{Bmatrix}\gamma_{yz}^s\\ \gamma_{xz}^s\end{Bmatrix}=\begin{Bmatrix}\dfrac{\partial w_s}{\partial y}\\ \dfrac{\partial w_s}{\partial x}\end{Bmatrix},\quad g(z)=1-\frac{df(z)}{dz} \tag{15}$$

2.3 Hamilton's principle

Now, Hamilton's principle can be defined as

$$\int_0^t \delta(U+V)dt=0 \tag{16}$$

where U and V account for strain energy and work done by external forces, respectively. The variation of strain energy is written as

$$\delta U=\int_V \sigma_{ij}\delta\varepsilon_{ij}dV=\int_V\begin{pmatrix}\sigma_x\delta\varepsilon_x+\sigma_y\delta\varepsilon_y+\sigma_{xy}\delta\gamma_{xy}\\ +\sigma_{yz}\delta\gamma_{yz}+\sigma_{xz}\delta\gamma_{xz}\end{pmatrix}dV \tag{17}$$

Substituting Eqs. (10)-(15) in Eq. (17) yields

$$\delta U=\int_0^L\begin{pmatrix}N_x\dfrac{\partial\delta u}{\partial x}-M_x^b\dfrac{\partial^2\delta w_b}{\partial x^2}-M_x^s\dfrac{\partial^2\delta w_s}{\partial x^2}+Q\dfrac{\partial w_s}{\partial x}\\ +N_y\dfrac{\partial\delta v}{\partial y}-M_y^b\dfrac{\partial^2\delta w_b}{\partial y^2}-M_y^s\dfrac{\partial^2\delta w_s}{\partial y^2}\\ +N_{xy}\left(\dfrac{\partial\delta u}{\partial y}+\dfrac{\partial\delta v}{\partial x}\right)-2M_{xy}^b\dfrac{\partial^2\delta w_b}{\partial x\partial y}\\ -2M_{xy}^s\dfrac{\partial^2\delta w_s}{\partial x\partial y}+Q_{yz}\dfrac{\partial\delta w_s}{\partial y}+Q_{xz}\dfrac{\partial\delta w_s}{\partial x}\end{pmatrix}d\lambda \tag{18}$$

In which the variables introduced in arriving at the last expression are defined as follows

$$\left[N_i,M_i^b,M_i^b\right]=\int_A[1,z,f(z)]\sigma_i dA,\quad i=(x,y,xy) \tag{19}$$

$$Q_i=\int_A g(z)\sigma_i dA,\quad i=(xz,yz) \tag{20}$$

Now, the first variation of work done by applied forces can be stated as

$$\delta V=\int_0^L\begin{pmatrix}(N_x^0+N_x^T)\dfrac{\partial\delta(w_b+w_s)}{\partial x}\dfrac{\partial(w_b+w_s)}{\partial x}\\ -k_w\delta(w_b+w_s)+k_p+\dfrac{\partial^2\delta(w_b+w_s)}{\partial x^2}\\ +\left(N_y^0+N_y^T\right)\dfrac{\partial\delta(w_b+w_s)}{\partial y}\dfrac{\partial(w_b+w_s)}{\partial y}\\ +2\delta N_{xy}^0\dfrac{\partial(w_b+w_s)}{\partial x}\dfrac{\partial(w_b+w_s)}{\partial y}\end{pmatrix}dx \tag{21}$$

In above relations, $N_x^0{=}N_y^0{=}N_b$ are in-plane applied loads and k_w, k_p are elastic foundation parameters. In this study, it assumed that the nanocomposite plate is under a biaxial Buckling loading (N_b) and thermal loading ($N_x^T=N_y^T=N^T$); also, the shear loading is ignored ($N_{xy}^0=0$). The thermal loading (N^T) can be defined as

$$N^T=\int_{-\frac{h}{2}}^{\frac{h}{2}}\left(\frac{E_{eff}}{1-\nu_{eff}}\,\alpha_{eff}\Delta T\right)dz \tag{22}$$

By Substituting Eqs. (18) and (21) into Eq. (16) and setting the coefficients of δu, δv, δw_b and δw_s to zero, the following Euler–Lagrange equation can be obtained

$$\frac{\partial N_x}{\partial x}+\frac{\partial N_{xy}}{\partial y}=0 \tag{23}$$

$$\frac{\partial N_{xy}}{\partial x}+\frac{\partial N_y}{\partial y}=0 \tag{24}$$

$$\begin{aligned}&\frac{\partial^2 M_x^b}{\partial x^2}+2\frac{\partial^2 M_{xy}^b}{\partial x\partial y}+\frac{\partial^2 M_y^b}{\partial y^2}+\frac{\partial Q}{\partial x}\\ &-(N_b+N^T)\nabla^2(w_b+w_s)-k_w(w_b+w_s)\\ &+k_p\nabla^2(w_b+w_s)=0\end{aligned} \tag{25}$$

$$\begin{aligned}&\frac{\partial^2 M_x^s}{\partial x^2}+2\frac{\partial^2 M_{xy}^s}{\partial x\partial y}+\frac{\partial^2 M_y^s}{\partial y^2}+\frac{\partial Q_{xy}}{\partial x}+\frac{\partial Q_{yz}}{\partial y}\\ &-(N_b+N^T)\nabla^2(w_b+w_s)-k_w(w_b+w_s)\\ &+k_p\nabla^2(w_b+w_s)=0\end{aligned} \tag{26}$$

In which ∇^2 is the Laplacian operator.

2.4 Constitutive equations

In this section, the stress-strain relations of isotropic materials are reviewed for the purpose of deriving the fundamental elastic equations of solids. Here, following constitutive equations in a thermal environment can be expressed as

$$\sigma_{ij}=C_{ijkl}\varepsilon_{kl} \tag{27}$$

where σ_{ij} and ε_{kl} are the components of second order stress and strain tensors, respectively; whereas, C_{ijkl} corresponds with the components of the fourth order elasticity tensor. Whenever extending the aforementioned equation for a shear deformable plate, the following relations can be reached

$$\begin{bmatrix}\sigma_{xx}\\ \sigma_{yy}\\ \sigma_{yz}\\ \sigma_{xz}\\ \sigma_{xy}\end{bmatrix}=\begin{bmatrix}Q_{11} & Q_{12} & 0 & 0 & 0\\ Q_{12} & Q_{22} & 0 & 0 & 0\\ 0 & 0 & Q_{44} & 0 & 0\\ 0 & 0 & 0 & Q_{55} & 0\\ 0 & 0 & 0 & 0 & Q_{66}\end{bmatrix}\begin{bmatrix}\varepsilon_{xx}\\ \varepsilon_{yy}\\ \varepsilon_{yz}\\ \varepsilon_{xz}\\ \varepsilon_{xy}\end{bmatrix} \tag{28}$$

where

$$Q_{11}=\frac{E_{eff}}{1-{\nu_{eff}}^2},\qquad Q_{12}=\nu_{eff}Q_{11},\\ Q_{22}=Q_{11},\qquad Q_{44}=Q_{55}=Q_{66}=G_{eff} \tag{29}$$

in which E_{eff} and G_{eff} denote the Young and shear moduli of the nanocomposite, respectively. Integrating from Eq. (28) over the cross-section area of the plate, the following equations can be written for the stress resultants

$$\begin{Bmatrix}N_X\\ N_y\\ N_{Xy}\end{Bmatrix}=\begin{pmatrix}A_{11} & A_{12} & 0\\ A_{21} & A_{22} & 0\\ 0 & 0 & A_{66}\end{pmatrix}\begin{Bmatrix}\dfrac{\partial u}{\partial x}\\ \dfrac{\partial v}{\partial y}\\ \dfrac{\partial u}{\partial y}+\dfrac{\partial v}{\partial x}\end{Bmatrix}+\begin{pmatrix}B_{11} & B_{12} & 0\\ B_{21} & B_{22} & 0\\ 0 & 0 & B_{66}\end{pmatrix}\begin{Bmatrix}-\dfrac{\partial^2 w_b}{\partial u^2}\\ -\dfrac{\partial^2 w_b}{\partial y^2}\\ -2\dfrac{\partial^2 w_b}{\partial x\partial y}\end{Bmatrix}+\begin{pmatrix}B_{11}^s & B_{12}^s & 0\\ B_{21}^s & B_{22}^s & 0\\ 0 & 0 & B_{66}^s\end{pmatrix}\begin{Bmatrix}-\dfrac{\partial^2 w_s}{\partial u^2}\\ -\dfrac{\partial^2 w_s}{\partial y^2}\\ -2\dfrac{\partial^2 w_s}{\partial x\partial y}\end{Bmatrix} \tag{30}$$

$$\begin{Bmatrix}M_x^b\\ M_y^b\\ M_{xy}^b\end{Bmatrix}=\begin{pmatrix}B_{11} & B_{12} & 0\\ B_{21} & B_{22} & 0\\ 0 & 0 & B_{66}\end{pmatrix}\begin{Bmatrix}\dfrac{\partial u}{\partial x}\\ \dfrac{\partial v}{\partial y}\\ \dfrac{\partial u}{\partial y}+\dfrac{\partial v}{\partial x}\end{Bmatrix}+\begin{pmatrix}D_{11} & D_{12} & 0\\ D_{21} & D_{22} & 0\\ 0 & 0 & D_{66}\end{pmatrix}\begin{Bmatrix}-\dfrac{\partial^2 w_b}{\partial u^2}\\ -\dfrac{\partial^2 w_b}{\partial y^2}\\ -2\dfrac{\partial^2 w_b}{\partial x\partial y}\end{Bmatrix} \tag{31}$$

$$+\begin{pmatrix}D_{11}^s & D_{12}^s & 0\\ D_{21}^s & D_{22}^s & 0\\ 0 & 0 & D_{66}^s\end{pmatrix}\begin{Bmatrix}-\dfrac{\partial^2 w_s}{\partial u^2}\\ -\dfrac{\partial^2 w_s}{\partial y^2}\\ -2\dfrac{\partial^2 w_s}{\partial x\partial y}\end{Bmatrix}$$

$$\begin{Bmatrix}M_x^s\\ M_y^s\\ M_{xy}^s\end{Bmatrix}=\begin{pmatrix}B_{11}^s & B_{12}^s & 0\\ B_{21}^s & B_{22}^s & 0\\ 0 & 0 & B_{66}^s\end{pmatrix}\begin{Bmatrix}\dfrac{\partial u}{\partial x}\\ \dfrac{\partial v}{\partial y}\\ \dfrac{\partial u}{\partial y}+\dfrac{\partial v}{\partial x}\end{Bmatrix}+\begin{pmatrix}D_{11}^s & D_{12}^s & 0\\ D_{21}^s & D_{22}^s & 0\\ 0 & 0 & D_{66}^s\end{pmatrix}\begin{Bmatrix}-\dfrac{\partial^2 w_b}{\partial u^2}\\ -\dfrac{\partial^2 w_b}{\partial y^2}\\ -2\dfrac{\partial^2 w_b}{\partial x\partial y}\end{Bmatrix} \tag{32}$$

$$+\begin{pmatrix}H_{11}^s & H_{12}^s & 0\\ H_{21}^s & H_{22}^s & 0\\ 0 & 0 & H_{66}^s\end{pmatrix}\begin{Bmatrix}-\dfrac{\partial^2 w_s}{\partial u^2}\\ -\dfrac{\partial^2 w_s}{\partial y^2}\\ -2\dfrac{\partial^2 w_s}{\partial x\partial y}\end{Bmatrix}$$

$$\begin{Bmatrix}Q_x\\ Q_y\end{Bmatrix}=\begin{pmatrix}A_{44}^s & 0\\ 0 & A_{55}^s\end{pmatrix}\begin{Bmatrix}\dfrac{\partial w_s}{\partial x}\\ \dfrac{\partial w_s}{\partial y}\end{Bmatrix} \tag{33}$$

In Eqs. (30)-(33) the cross-sectional rigidities are given by following relations

$$\begin{Bmatrix}A_{11} & B_{11} & D_{11} & B_{11}^s & D_{11}^s & H_{11}^s\\ A_{12} & B_{12} & D_{12} & B_{12}^s & D_{12}^s & H_{12}^s\\ A_{66} & B_{66} & D_{66} & B_{66}^s & D_{66}^s & H_{66}^s\end{Bmatrix}\\ =\int_{-\frac{h}{2}}^{\frac{h}{2}}\frac{E_{eff}}{1-\nu_{eff}^2}(1,z,z^2,f(z),zf(z),f^2(z))\begin{Bmatrix}1\\ \nu_{eff}\\ \dfrac{1-\nu_{eff}}{2}\end{Bmatrix}dz \tag{34}$$

$$(A_{22},B_{22},D_{22},B_{22}^s,D_{22}^s,H_{22}^s)\\ =(A_{11},B_{11},D_{11},B_{11}^s,D_{11}^s,H_{11}^s) \tag{35}$$

$$A_{44}^s=A_{55}^s=\int_{-\frac{h}{2}}^{\frac{h}{2}}\frac{E_{eff}}{2(1+\nu_{eff})}(g^2(z))\,dz \tag{36}$$

By substituting Eqs. (30)–(33) into Eqs. (23)-(26), the governing equations of nanocomposite plate can be directly written in terms of displacements (u, v, w_b, and w_s) as

$$A_{11}\frac{\partial^2 u}{\partial x^2}+(A_{12}+A_{66})\frac{\partial^2 v}{\partial x\partial y}+A_{66}\frac{\partial^2 u}{\partial y^2}-B_{11}\frac{\partial^3 w_b}{\partial x^3} \tag{37}$$

$$-(B_{12}+2B_{66})\frac{\partial^3 w_b}{\partial x\partial y^2}-B_s^{11}\frac{\partial^3 w_s}{\partial x^3}$$
$$-(B_{12}^s+2B_{66}^s)\frac{\partial^3 w_s}{\partial x\partial y^2}=0 \quad (37)$$

$$A_{22}\frac{\partial^2 v}{\partial y^2}+(A_{12}+A_{66})\frac{\partial^2 u}{\partial x\partial y}+A_{66}\frac{\partial^2 v}{\partial x^2}$$
$$-B_{11}\frac{\partial^3 w_b}{\partial x^3}-B_{22}\frac{\partial^3 w_b}{\partial y^3}-(B_{12}+2B_{66})\frac{\partial^2 w_b}{\partial x^2\partial y} \quad (38)$$
$$-B_s^{22}\frac{\partial^3 w_s}{\partial y^3}-(B_{12}^s+2B_{66}^s)\frac{\partial^3 w_s}{\partial x^2\partial y}=0$$

$$B_{11}\frac{\partial^3 u}{\partial x^3}+(B_{12}+2B_{66})\frac{\partial^3 u}{\partial x\partial y^2}+B_{22}\frac{\partial^3 v}{\partial y^3}$$
$$-(B_{12}+2B_{66})\frac{\partial^3 v}{\partial x^2\partial y}-D_{11}\frac{\partial^4 w_b}{\partial x^4}$$
$$-2(D_{12}+2D_{66})\frac{\partial^4 w_b}{\partial x^2\partial y^2}-D_{22}\frac{\partial^4 w_b}{\partial y^4}-D_{11}^s\frac{\partial^4 w_s}{\partial x^4} \quad (39)$$
$$-2(D_{12}^s+2D_{66}^s)\frac{\partial^4 w_s}{\partial x^2\partial y^2}-D_{22}^s\frac{\partial^4 w_s}{\partial y^4}$$
$$+(k_p-N_b-N^T)\nabla^2(w_b+w_s)-k_w(w_b+w_s)=0$$

$$B_{11}^s\frac{\partial^3 u}{\partial x^3}+(B_{12}^s+2B_{66}^s)\frac{\partial^3 u}{\partial x\partial y^2}+B_{22}^s\frac{\partial^3 v}{\partial y^3}$$
$$-(B_{12}^s+2B_{66}^s)\frac{\partial^3 v}{\partial x^2\partial y}-D_{11}^s\frac{\partial^4 w_b}{\partial x^4}$$
$$-2(D_{12}^s+2D_{66}^s)\frac{\partial^4 w_b}{\partial x^2\partial y^2}-D_{22}^s\frac{\partial^4 w_b}{\partial y^4}-H_{11}^s\frac{\partial^4 w_s}{\partial x^4} \quad (40)$$
$$-2(H_{12}^s+2H_{66}^s)\frac{\partial^4 w_s}{\partial x^2\partial y^2}-H_{22}^s\frac{\partial^4 w_s}{\partial y^4}$$
$$+(k_p-N_b-N^T)\nabla^2(w_b+w_s)-k_w(w_b+w_s)=0$$

3. Solution procedure

Here, on the basis of the Navier method, an analytical solution of the governing equations for buckling of a simply supported FG-GOPR nanocomposite plate is presented. To satisfy the simply supported boundary condition, the displacement fields are in the following form

$$u=\sum_{m=1}^{\infty}\sum_{n=1}^{\infty}U_{mn}\,cos(\alpha x)\,sin(\beta y)\,e^{i\omega_n t} \quad (41)$$

$$v=\sum_{m=1}^{\infty}\sum_{n=1}^{\infty}V_{mn}\,sin(\alpha x)\,cos(\beta y)\,e^{i\omega_n t} \quad (42)$$

$$w_b=\sum_{m=1}^{\infty}\sum_{n=1}^{\infty}W_{bmn}\,sin(\alpha x)\,sin(\beta y)\,e^{i\omega_n t} \quad (43)$$

$$w_s=\sum_{m=1}^{\infty}\sum_{n=1}^{\infty}W_{smn}\,sin(\alpha x)\,sin(\beta y)\,e^{i\omega_n t} \quad (44)$$

Where U_{mn}, V_{mn}, W_{bmn} and W_{smn} are the unknown Fourier coefficients and $\alpha=\frac{m\pi}{a}$, $\beta=\frac{n\pi}{b}$. Once Eqs. (41)-(44) are inserted in Eqs. (37)-(40) respectively, the following relation can be obtained

$$\left\{\begin{pmatrix}k_{11}&k_{12}&k_{13}&k_{14}\\k_{21}&k_{22}&k_{23}&k_{24}\\k_{31}&k_{32}&k_{33}&k_{34}\\k_{41}&k_{42}&k_{43}&k_{44}\end{pmatrix}\right\}\begin{Bmatrix}U_{mn}\\V_{mn}\\W_{bmn}\\W_{smn}\end{Bmatrix}=0 \quad (45)$$

in which K is stiffness matrix. The k_{ij} arrays can be calculated in the following form

$$\begin{aligned}
k_{11}&=-(A_{11}\alpha^2+A_{66}\beta^2),\\
k_{12}&=-\alpha\beta(A_{12}+A_{66}),\\
k_{13}&=\alpha^3B_{11}+\alpha\beta^2(B_{12}+2B_{66})\\
k_{14}&=B_{11}^s\alpha^3+\alpha\beta^2(B_{12}^s+2B_{66}^s),\\
k_{21}&=k_{12},\\
k_{22}&=-(\beta^2A_{22}+\alpha^2A_{66})\\
k_{23}&=\beta^3B_{22}+\beta\alpha^2(B_{12}+2B_{66}),\\
k_{24}&=\beta^3B_{22}^s+\beta\alpha^2(B_{12}^s+2B_{66}^s),\\
k_{31}&=k_{13}\\
k_{32}&=k_{23},\\
k_{33}&=-(\alpha^4D_{11}+2\alpha^2\beta^2(D_{12}+2D_{66})+\beta^4D_{22}\\
&\quad+k_w+(\alpha^2+\beta^2)\left(k_p-N_b-N^T\right)\\
k_{34}&=-(\alpha^4D_{11}^s+2\alpha^2\beta^2(D_{12}^s+2D_{66}^s)+\beta^4D_{22}^s\\
&\quad+k_w+(\alpha^2+\beta^2)\left(k_p-N_b-N^T\right)\\
k_{42}&=k_{24},\\
k_{43}&=k_{34},\\
k_{41}&=k_{14}\\
k_{44}&=-(\alpha^4H_{11}^s+2\alpha^2\beta^2(H_{12}^s+2H_{66}^s)+\beta^4H_{22}^s\\
&\quad+k_w+(\alpha^2+\beta^2)(A^s+k_p-N_b-N^T)
\end{aligned} \quad (46)$$

4. Types of thermal loading

4.1 Uniform temperature rise (*UTR*)

By assuming an FG-GOPR nanocomposite plate at reference temperature T_0 and final temperature T, the uniform temperature change can be defined as

$$\Delta T=T-T_0$$

4.2 Linear temperature rise (*LTR*)

The temperature of a FG-GOPR nanocomposite plate can be raised linearly through the thickness through the following formulation by considering the plate to be thin enough

$$T=T_0+\Delta T(\frac{1}{2}+\frac{z}{h})$$

Where T is the final temperature and T_0 is the reference temperature of the plate.

4.3 Sinusoidal temperature rise (STR)

When the plate is subjected to sinusoidal temperature rise, the temperature distribution throughout the thickness

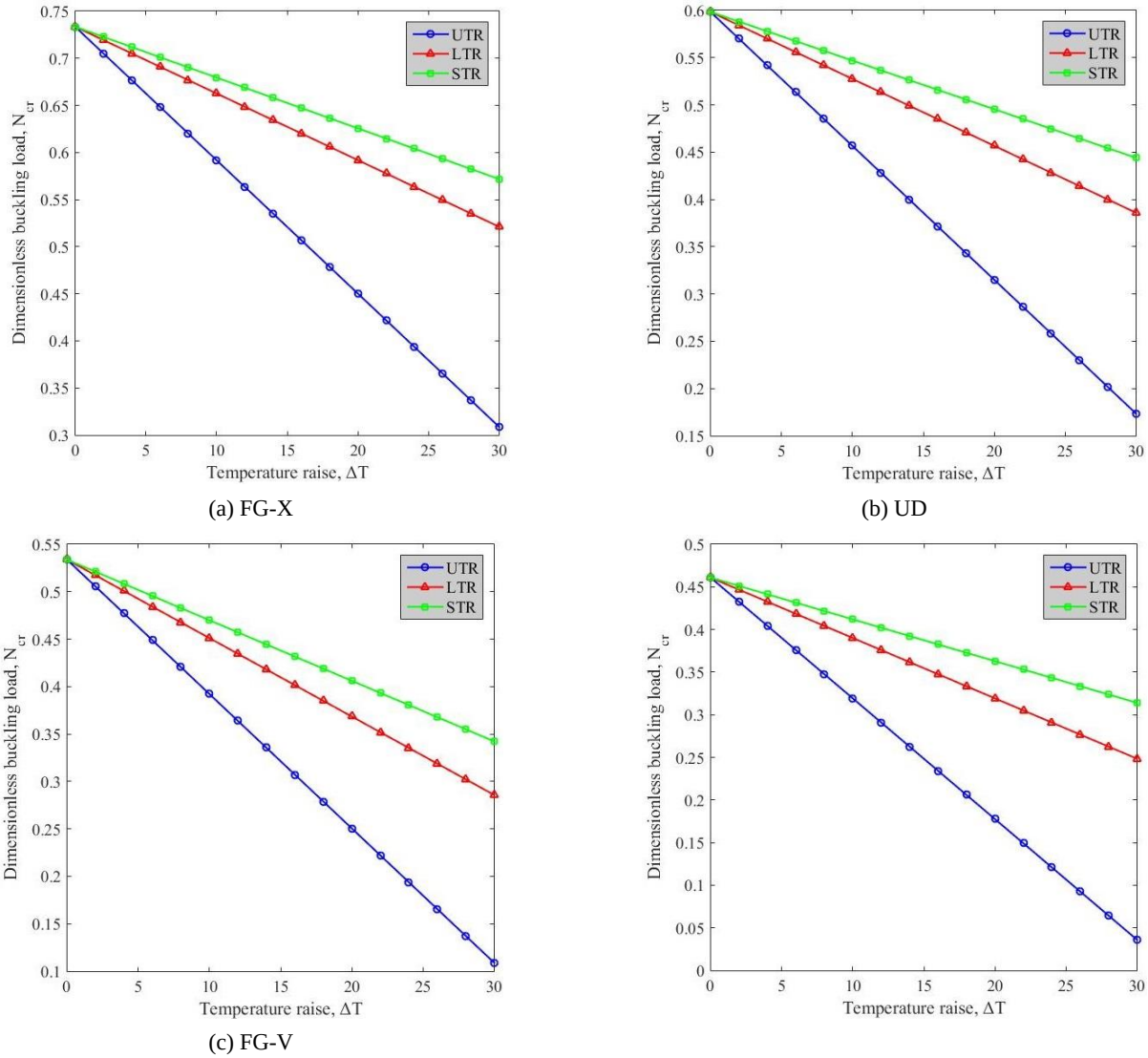

Fig. 1 Variation of dimenshpgionless buckling load of a GOPR nanocomposite plate versus temperature raise for (a) FG-X; (b) UD; (c) FG-V; and (d) FG-O distribution type with respect to various types of thermal loading through the thickness

can be expressed as

$$T = T_0 + \Delta T\left(1 - cos\frac{\pi}{2}\left(\frac{1}{2} + \frac{z}{h}\right)\right)$$

Where $\Delta T = T - T_0$ is the temperature change.

5. Numerical results and discussion

Through this section, the effects of various parameters such as three kinds of thermal loading, GOPs' weight fraction, aspect ratio, length to thickness ratio, two kinds of elastic foundation and different types of GOPs' distribution on the critical buckling loads of GOPR nanocomposite plates will be figured out by interpreting the numerical results stated in the following. For the sake of simplicity, the dimensionless form of the buckling load, Winkler and Pasternak parameters are defined in the following form:

$$K_w = k_w\frac{a^4}{D_C}, \quad K_p = k_p\frac{a^2}{D_C},$$

$$N_{Cr} = N_b\frac{a^2}{100D_C}, \quad D_C = \frac{E_M h^3}{12(1-\nu_M^2)}$$

The static deflection of the CNT reinforced nanocomposite square plates with the SSSS boundary condition and four types of nanofillers' distribution are obtained via present model and compared with those reported by (REFERENCE) in Table 1.

Fig. 1 gives the variation of critical buckling load against temperature raise by considering different types of thermal loading for various types of GOPs' distribution including uniform distribution (UD), FG-O, FG-V and FG-X. According to this figure, the critical buckling loads start to decrease due to the stiffness reduction caused by temperature raise. However, it is clear that the structure under STR has higher range of dimensionless buckling load

Table 1 Comparison of the dimensionless static deflection responses of CNTR plates with simply-supported boundary conditions (V^*_{CNT} = 0.11, q_0 = 0.1 MPa)

b/*h*	Distribution pattern	Zhu *et al*. (2012)	Present
10	UD	3.739e-3	3.717e-3
	FG-V	4.466e-3	4.463e-3
	FG-O	5.230e-3	5.2484e-3
	FG-X	3.177e-3	3.150e-3
20	UD	3.628e-2	3.644
	FG-V	4.879e-2	4.874e-2
	FG-O	6.155e-2	6.135e-2
	FG-X	2.701e-2	2.713e-2
50	UD	1.155	1.164
	FG-V	1.653	1.651
	FG-O	2.157	2.123
	FG-X	0.79	0.804

followed by LTR and UTR, respectively. On the other hand, UTR makes the plate more flexible and causes higher stiffness reduction in the plate compared with the other types of temperature raise. As illustrated in Fig. 1, plates with FG-O distribution pattern for the nanofillers have the lowest value of dimensionless buckling load, whereas, FG-X ones possess the highest value.

To investigate the influences of the foundation parameters on the dimensionless buckling load of GOPR nanocomposite plates, the variation of dimensionless buckling load is plotted against Winkler and Pasternak coefficients in Figs. 2 and 3, respectively for each GOP distribution pattern by considering three types of temperature raise. As shown in Figs. 2 and 3, for the all types of temperature rise, an increase in the foundation parameters' stiffness will improve the critical buckling load of the nanocomposite plate gradually. Moreover, comparing these figures together, it can be also concluded that the Pasternak parameter can affect the structure fantastically more than Winkler parameter. From this sense, it can be

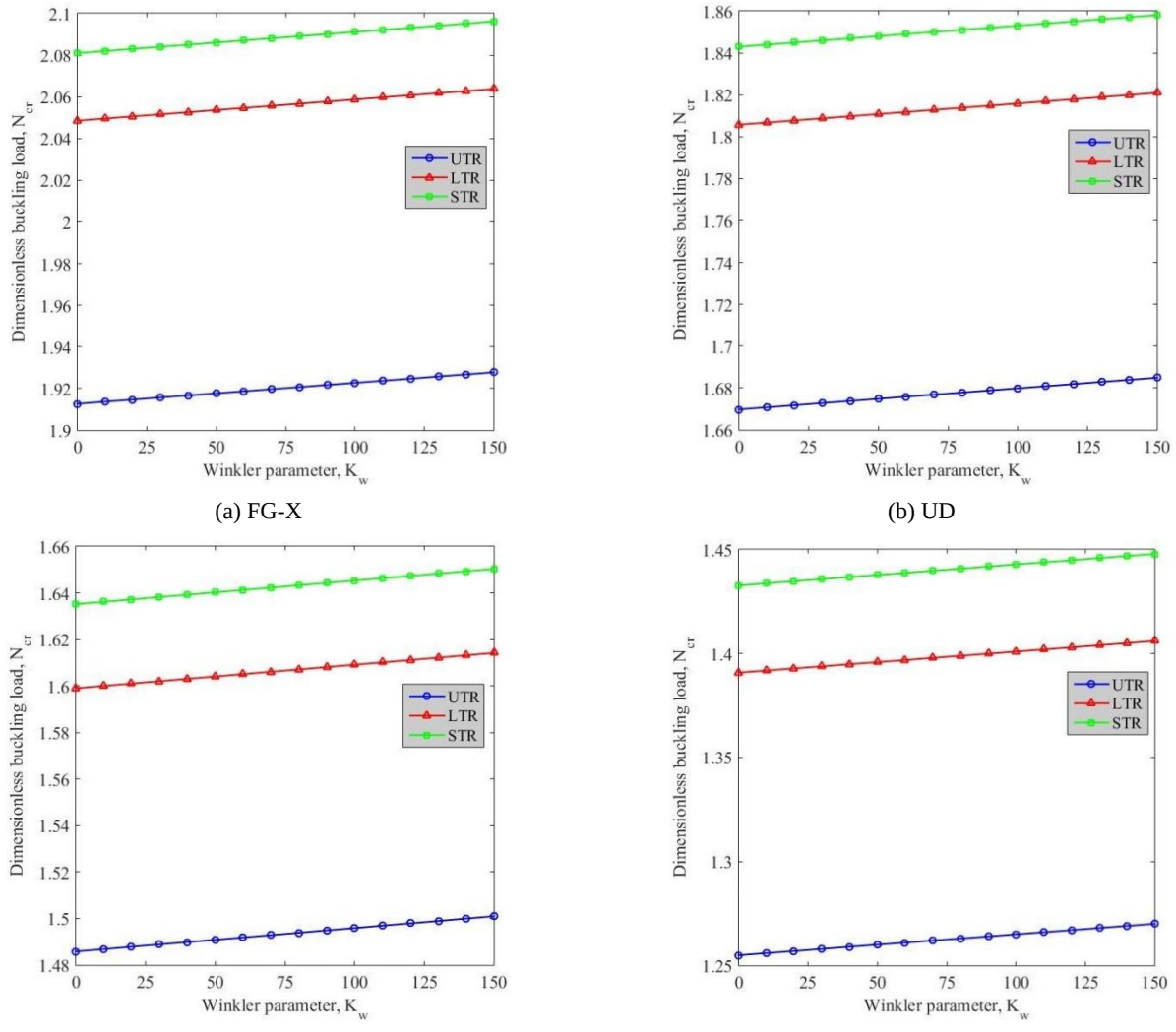

(a) FG-X (b) UD

(c) FG-V

Fig. 2 Variation of critical buckling load versus Winkler coefficient for (a) FG-X; (b) UD; (c) FG-V; and (d) FG-O distribution type with respect to various types of thermal loading through the thicknes

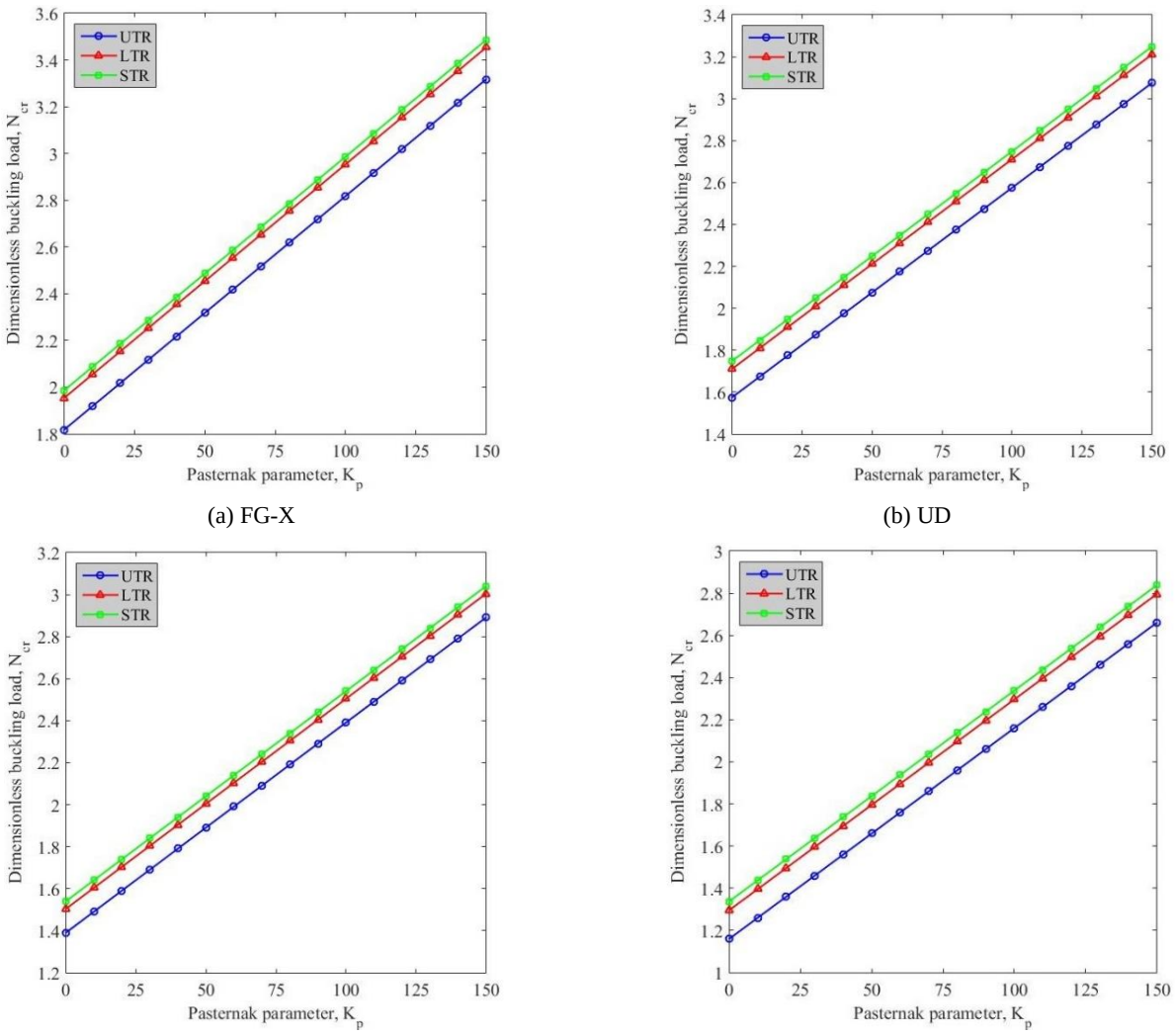

(a) FG-X (b) UD

(c) FG-V (d) FG-O

Fig. 3 Variation of critical buckling load versus Pasternak coefficient for (a) FG-X; (b) UD; (c) FG-V; and (d) FG-O distribution type with respect to various types of thermal loading through the thickness

found that Pasternak parameter can improve the buckling behavior of the GOPR nanocomposite plates more efficiently than Winkler parameter. Also, it is interesting to note that applying a STR makes the structure less flexible, hence, the critical buckling loads of the plates under this type of thermal loading have higher range in comparison with other types of thermal loading. Also, as same as Fig. 1, the nanocomposite plate with X-distribution endures higher buckling loads.

Figs. 4 and 5 show the variation of critical buckling load versus aspect ratio by exposing the plate to different types of thermal loadings in order to compare the buckling behavior of the structure with and without thermal effects. These figures are consisted of four parts for each type of GOP distribution. In these figures, two values are assigned to the temperature raise. It can be clearly observed that in Fig. 4, with lower value of temperature change ($\Delta T = 10$), increment in the amount of aspect ratio can appropriately withstand with the thermal effects which causes an increase in the critical buckling load even under thermal loading. However, in Fig. 5, with higher value of temperature change ($\Delta T = 20$), only the plate with X-distribution of the GOPs can tolerate buckling load under every type of thermal loading. Also, as seen in Figs. 5(b), (c) and (d), UTR has a huge softening effect on the structure in a way that nothing is able to prevent the structure's failure. In addition, it is found from these two figures that STR provides higher range of dimensionless buckling loads and after that LTR is more desirable than UTR. As it is obvious from these two figures, without applying thermal effects, the plate undergoes larger range of dimensionless buckling loads as a result of applying a growth in aspect ratio values. It would be understandable form the interoperating of these figures that only X-distribution type of reinforcements can tolerate the thermal loadings with UTR.

The next step is to analyze the effects of GOPs' weight fraction, different types of temperature rise and elastic foundation on the critical buckling loads in detail. The variation of the dimensionless buckling loads against GOPs' weight fraction is presented in Fig. 6 for various types of GOP distribution. The values of temperature change and elastic foundation coefficient are considered to be constant

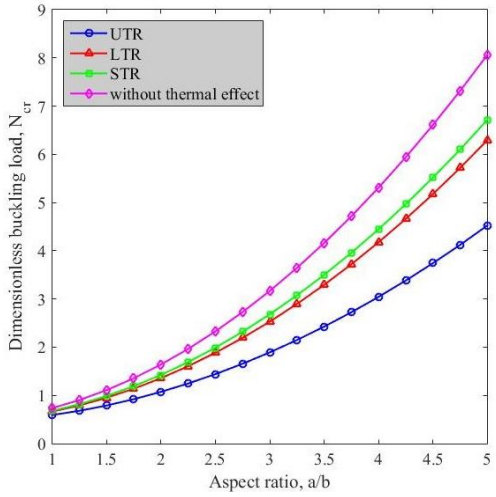

(a) FG-X

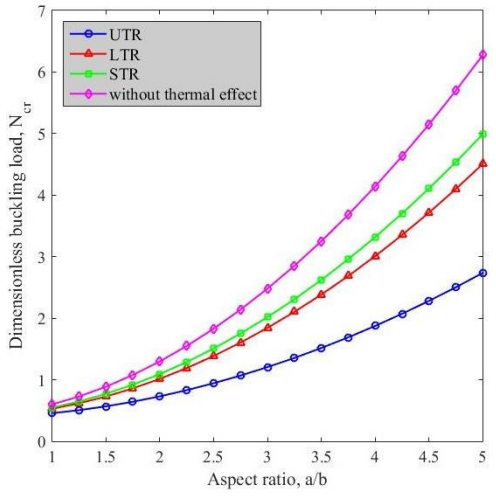

(b) UD

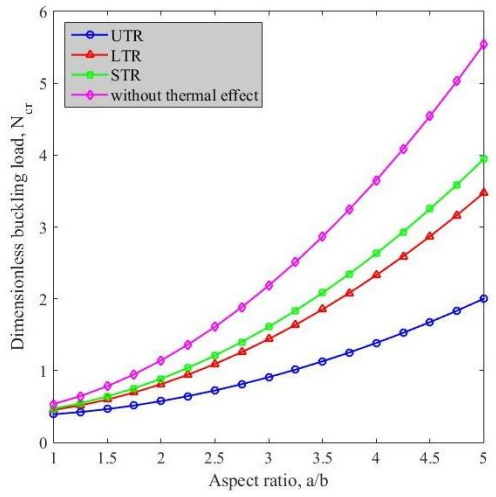

(c) FG-V

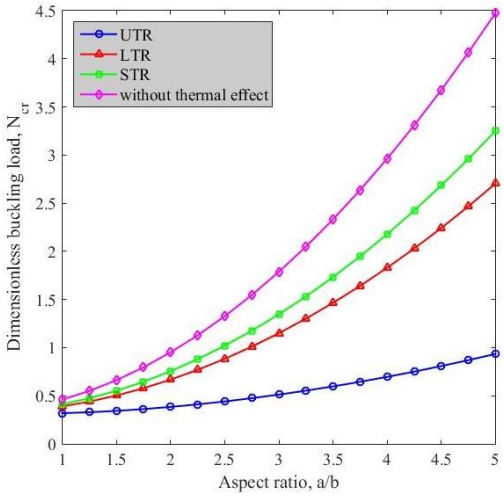

(d) FG-O

Fig. 4 Variation of critical buckling load versus plate aspect ratio for (a) FG-X; (b) UD; (c) FG-V; and (d) FG-O distribution type with respect to various types of thermal loading through the thickness by considering the amount of temperature change $\Delta T = 10K$

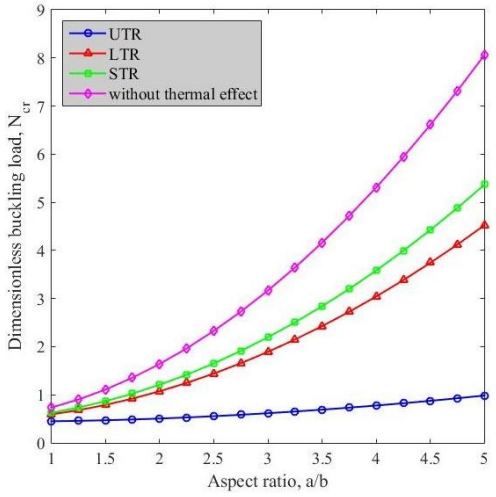

(a) FG-X

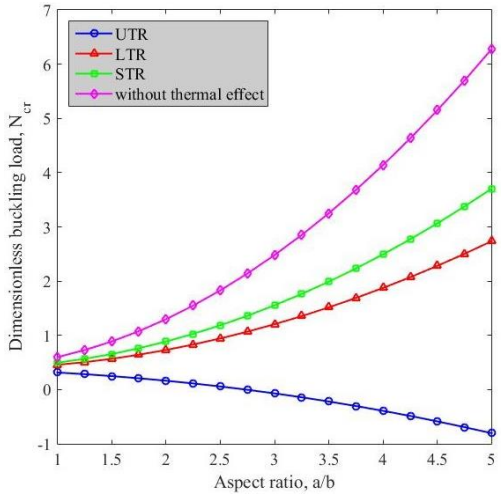

(b) UD

Fig. 5 Variation of critical buckling load versus plate aspect ratio for (a) FG-X; (b) UD; (c) FG-V; and (d) FG-O distribution type with respect to various types of thermal loading through the thickness by considering the amount of temperature change $\Delta T = 20K$

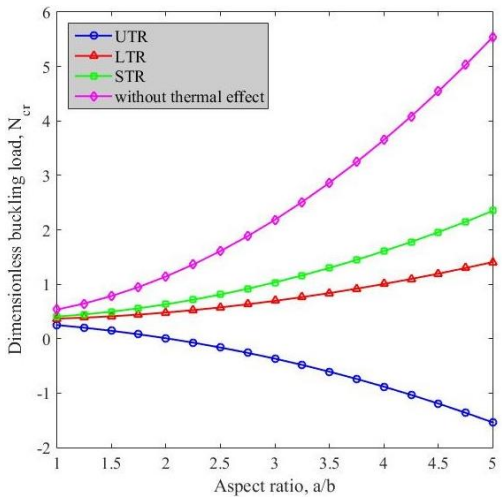

(c) FG-V

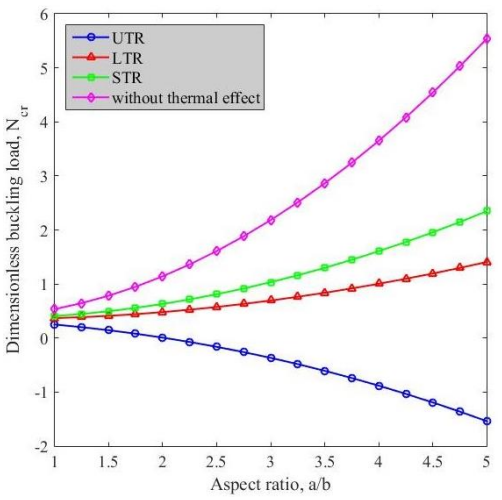

(d) FG-O

Fig. 5 Continued

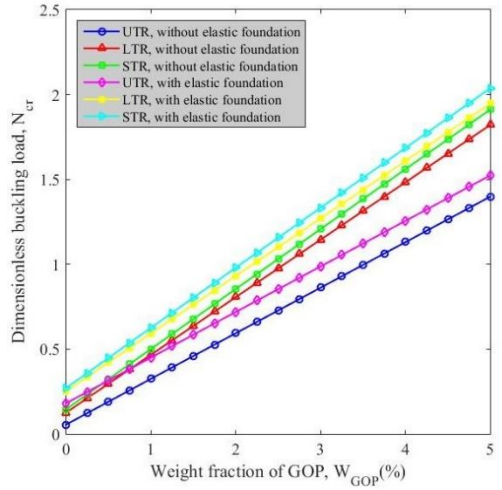

(a) FG-X

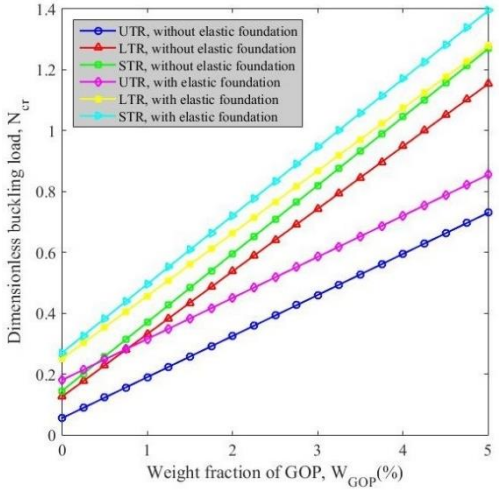

(b) UD

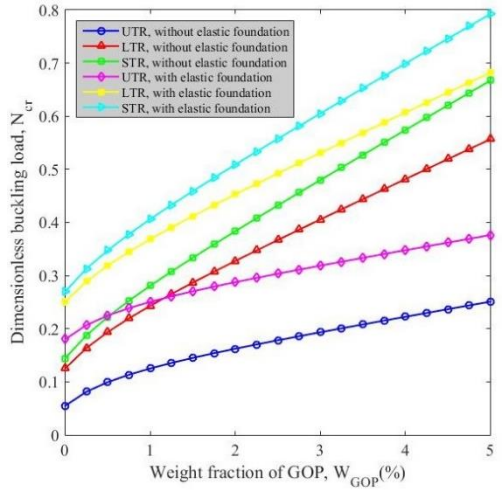

(c) FG-V

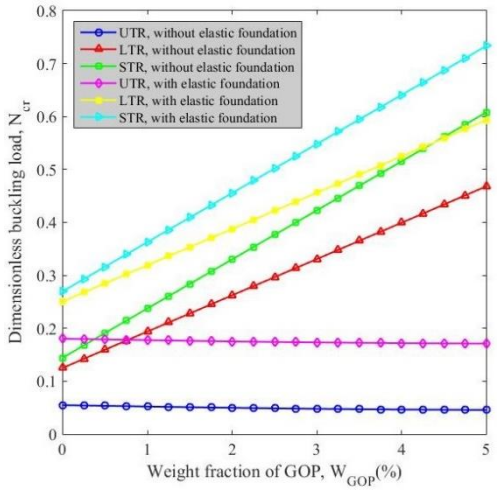

(d) FG-O

Fig. 6 Variation of dimensionless buckling load of a GOPR nanocomposite plate versus weight fraction of GOPs for (a) FG-X; (b) UD; (c) FG-V; and (d) FG-O distribution type with respect to various types of thermal loading through the thickness as well as the influence of elastic foundation

for all of the included subfigures. It can be evidently deduced from Fig. 6 that for each type of thermal loading and GOP distribution, an increase in the magnitude of GOPs' weight fraction overcomes the thermal effects except in Fig. 6(d). Hence, the critical buckling loads increase during the addition of the GOPs' weight fraction for the X, U and V distribution. According to the figure, the plate with elastic foundation under uniform type of thermal loading (UTR) has lower range of critical buckling load compared to the plate without elastic foundation under LTR or STR thermal loadings; means, the thermal loading with UTR prevails over the elastic foundation effects. By analyzing the plots of Fig. 6(d) in detail, for the O-distribution type, it can be figured out that an increase in the amount of weight fraction generates a decrease in the dimensionless buckling loads of the plate under UTR. This trend reveals that in such cases the softening influence of thermal expansion of the nanoparticles defeats the stiffness enhancement which is generated from dispersing nanoparticles in the media.

Fig. 7 shows the comparison between the buckling behaviors of the GOPR nanocomposite plates against length-to-thickness ratio with various types of GOP distribution for both thermally affected and without thermal effect conditions. As illustrated in this figure, for all types of GOPs' distribution, the reduction range of the buckling loads under UTR is remarkably higher than other types of thermal loading followed by LTR and STR. In other words, the structure can be exposed to higher temperatures by applying the STR. Also, by neglecting the thermal effects as seen in Fig. 7(d), the influence of the length-to-thickness ratio on critical buckling of the plate would be negligible.

To investigate how the GOPs' negative coefficient of thermal expansion affect the structure, the variation of the dimensionless buckling load of the plate is plotted versus length-to-thickness ratio with respect to different values of GOPs' weight fraction and various types of thermal loadings. From Fig. 8c and 8d, by comparing UTR type of thermal loading with two different values of GOPs' weigh fraction, it was expected that the plate with higher amount of GOPs' weight fraction should possess greater dimensionless buckling load in the highest rate of length-to-thickness ratio (a/h = 40) but as seen, it doesn't happen in

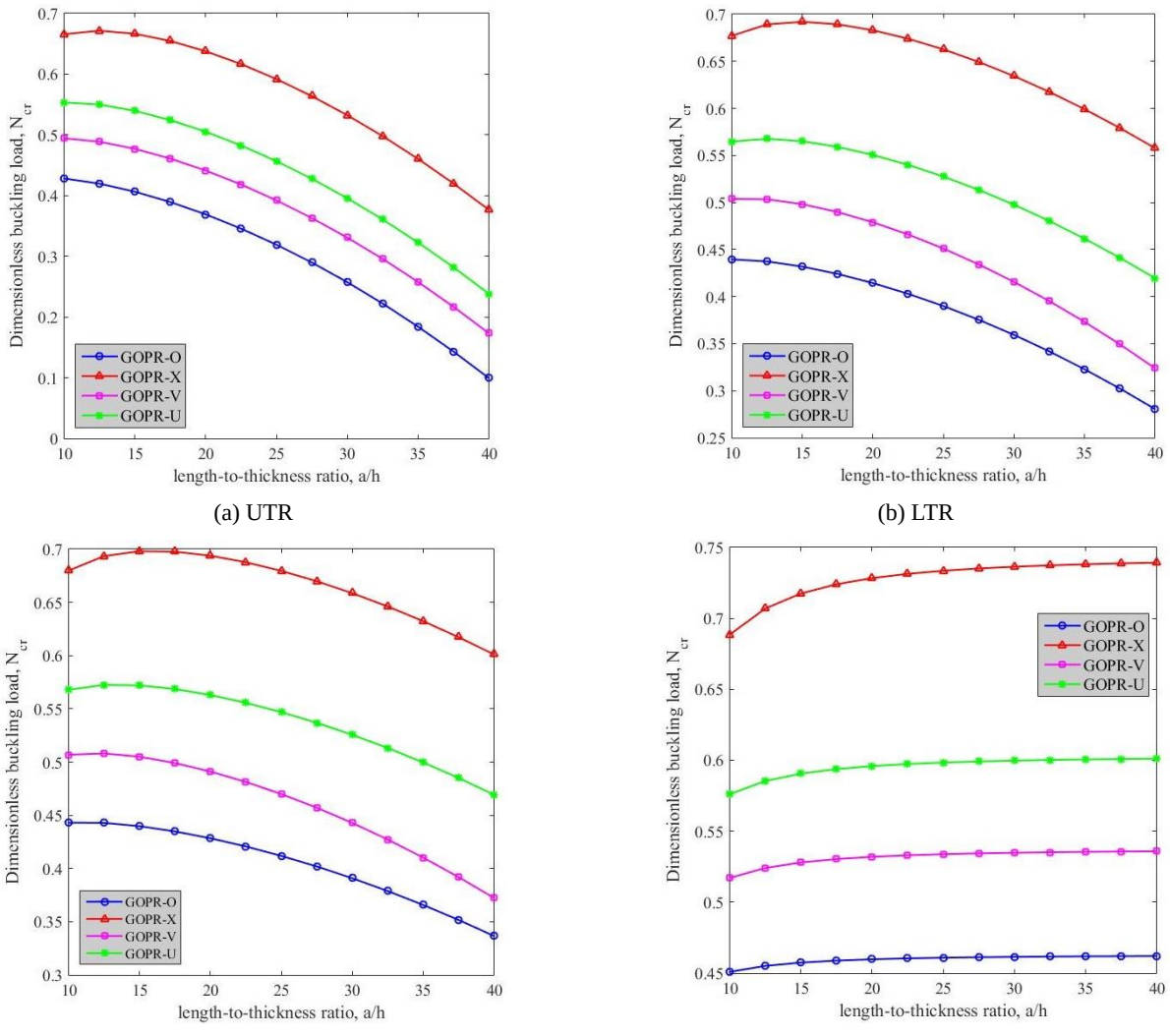

(a) UTR (b) LTR

(c) STR (d) Without thermal effect

Fig. 7 Variation of critical buckling load versus plate length-to-thickness ratio for (a) UTR; (b) LTR; (c) STR; and (d) without thermal effect with respect to various types of GOPs' distribution

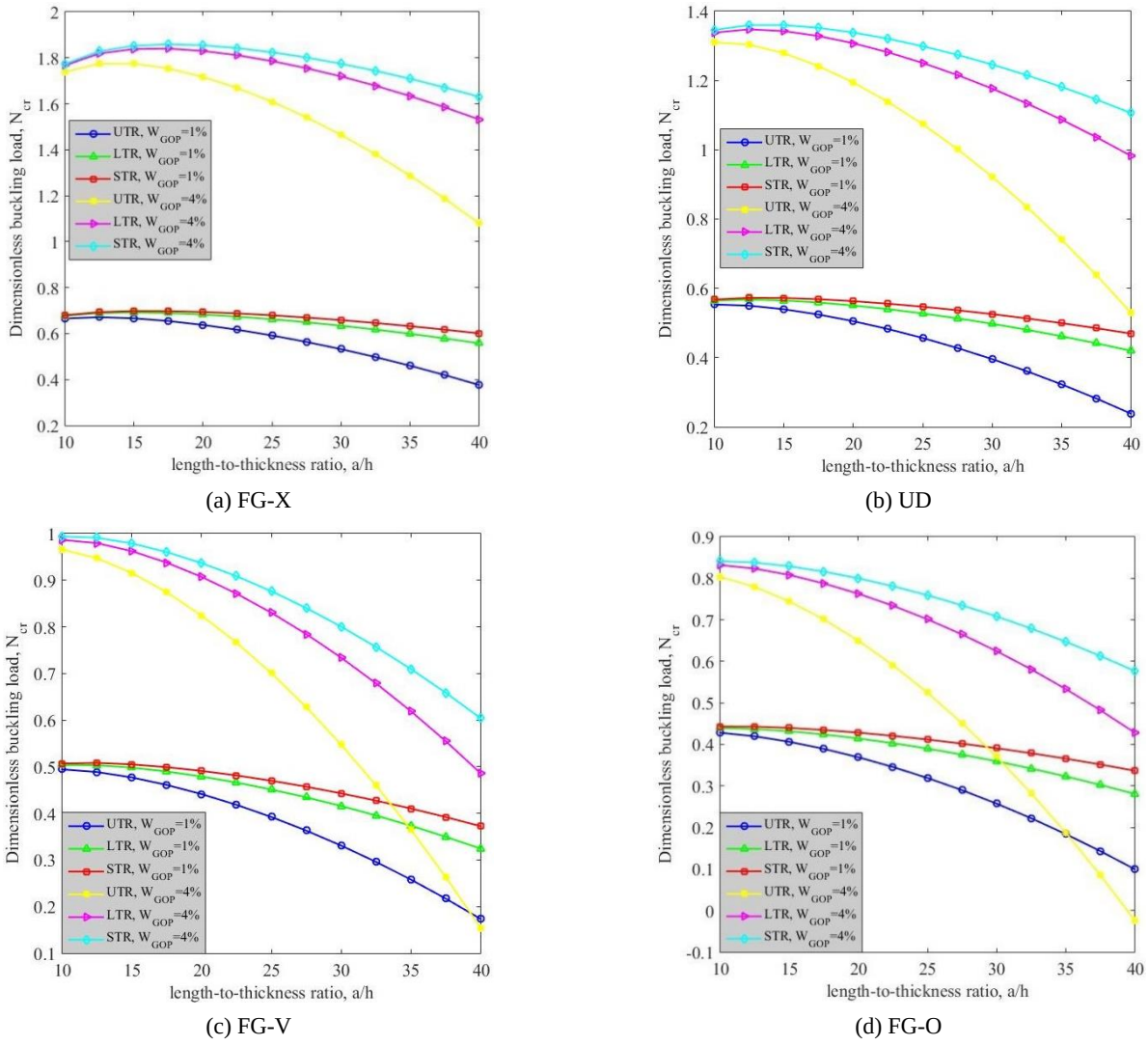

(a) FG-X (b) UD

(c) FG-V (d) FG-O

Fig. 8 Variation of dimensionless buckling load of a GOPR nanocomposite plate versus plate length-to-thickness ratio for (a) FG-X; (b) UD; (c) FG-V; and (d) FG-O distribution type with respect to various types of thermal loading through the thickness as well as the influence of GOPs' weight fraction

this figure and an addition in the amount of GOPs' weight fraction causes a reduction in the value of dimensionless buckling load. It can be inferred from this sense that the GOPs' negative coefficient of thermal expansion is the reason of this reverse trend. Also, as it was mentioned in the previous figures, the UTR causes significant reduction in the stiffness of the structure.

6. Conclusion

The thermal-buckling response of the FG-GOPR nanocomposite plates resting on the elastic substrate was investigated here. Various types of thermal effects were applied to the structure through the different types of temperature rises including uniform, linear and sinusoidal. Halpin-Tsai micromechanical scheme was employed to estimate the material properties of the plates with the aim of reinforcing the nanocomposite plates with uniform and three FG types of GOP distribution through the thickness. The governing equations were obtained on the basis of a refined higher order plate theory and then solved analytically via Navier method. According to the graphical results, the following highlights were obtained:

- It was discovered that although resting the structure on elastic foundation improves the stiffness of the structure, uniform thermal effect influences the structure in the way that even by embedding the plate on an elastic foundation, the structure cannot withstand under uniform type of thermal loading in higher range of temperature change.
- It was found that the nanocomposite plate under STR has higher range of dimensionless buckling loads followed by LTR and UTR, respectively.
- It was also revealed that buckling loads increase gradually as aspect ratio grows which is meant that the more the plate is got out from the square model, the plate gets higher values of dimensionless buckling loads.

- It is deduced that the most efficient type of GOP distribution is the X one followed by U, V and O distributions type.
- It is obvious that an increase in the amount of GOPs' weight fraction should significantly improve the buckling performances of GOPR nanocomposite plates but, it was inferred that the critical buckling loads of the plate with O-distribution will be unexpectedly decreased through the increment of the GOPs' weight fraction under uniform thermal loading according to the GOPs' negative coefficient of thermal expansion.
- It was found that length-to-thickness ratio has negligible effect on the critical buckling loads of a GOPR nanocomposite plate.

References

Abdelaziz, H.H., Meziane, M.A.A., Bousahla, A.A., Tounsi, A., Mahmoud, S. and Alwabli, A.S. (2017), "An efficient hyperbolic shear deformation theory for bending, buckling and free vibration of FGM sandwich plates with various boundary conditions", *Steel Compos. Struct., Int. J.*, **25**(6), 693-704. https://doi.org/10.12989/scs.2017.25.6.693

Akgoz, B. and Civalek, O. (2013), "Buckling analysis of linearly tapered micro-columns based on strain gradient elasticity", *Struct. Eng. Mech., Int. J.*, **48**(2), 195-205. https://doi.org/10.12989/sem.2013.48.2.195

Anlas, G. and Göker, G. (2001), "Vibration analysis of skew fibre-reinforced composite laminated plates", *J. Sound Vib.*, **242**, 265-276. https://doi.org/10.1006/jsvi.2000.3366

Arani, A.G., Maghamikia, S., Mohammadimehr, M. and Arefmanesh, A. (2011), "Buckling analysis of laminated composite rectangular plates reinforced by SWCNTs using analytical and finite element methods", *J. Mech. Sci. Technol.*, **25**, 809-820. https://doi.org/10.1007/s12206-011-0127-3

Arefi, M., Bidgoli, E.M.-R., Dimitri, R., Bacciocchi, M. and Tornabene, F. (2019), "Nonlocal bending analysis of curved nanobeams reinforced by graphene nanoplatelets", *Compos. Part B: Eng.*, **166**, 1-12. https://doi.org/10.1021/nl0731872

Bakhadda, B., Bouiadjra, M.B., Bourada, F., Bousahla, A.A., Tounsi, A. and Mahmoud, S. (2018), "Dynamic and bending analysis of carbon nanotube-reinforced composite plates with elastic foundation", *Wind Struct., Int. J.*, **27**(5), 311-324. https://doi.org/10.12989/was.2018.27.5.311

Balandin, A.A., Ghosh, S., Bao, W., Calizo, I., Teweldebrhan, D., Miao, F. and Lau, C.N. (2008), "Superior thermal conductivity of single-layer graphene", *Nano Letters*, **8**, 902-907. https://doi.org/10.1021/nl0731872

Baltacıoğlu, A., Civalek, Ö., Akgöz, B. and Demir, F. (2011), "Large deflection analysis of laminated composite plates resting on nonlinear elastic foundations by the method of discrete singular convolution", *Int. J. Press. Vessels Pip.*, **88**, 290-300. https://doi.org/10.1016/j.ijpvp.2011.06.004

Barati, M.R. (2017), "Nonlocal-strain gradient forced vibration analysis of metal foam nanoplates with uniform and graded porosities", *Adv. Nano Res., Int. J.*, **5**(4), 393-414. https://doi.org/10.12989/anr.2017.5.4.393

Barati, M.R. and Zenkour, A.M. (2017), "Post-buckling analysis of refined shear deformable graphene platelet reinforced beams with porosities and geometrical imperfection", *Compos. Struct.*, **181**, 194-202. https://doi.org/10.1016/j.compstruct.2017.08.082

Bellifa, H., Benrahou, K.H., Bousahla, A.A., Tounsi, A. and Mahmoud, S. (2017), "A nonlocal zeroth-order shear deformation theory for nonlinear postbuckling of nanobeams", *Struct. Eng. Mech., Int. J.*, **62**(6), 695-702. https://doi.org/10.12989/sem.2017.62.6.695

Bouadi, A., Bousahla, A.A., Houari, M.S.A., Heireche, H. and Tounsi, A. (2018), "A new nonlocal HSDT for analysis of stability of single layer graphene sheet", *Adv. Nano Res., Int. J.*, **6**(2), 147-162. https://doi.org/10.12989/anr.2018.6.2.147

Bouhadra, A., Tounsi, A., Bousahla, A.A., Benyoucef, S. and Mahmoud, S. (2018), "Improved HSDT accounting for effect of thickness stretching in advanced composite plates", *Struct. Eng. Mech., Int. J.*, **66**(1), 61-73. https://doi.org/10.12989/sem.2018.66.1.061

Bourada, F., Bousahla, A.A., Bourada, M., Azzaz, A., Zinata, A. and Tounsi, A. (2019), "Dynamic investigation of porous functionally graded beam using a sinusoidal shear deformation theory", *Wind Struct., Int. J.*, **28**(1), 19-30. https://doi.org/10.12989/was.2019.28.1.019

Cai, W., Moore, A.L., Zhu, Y., Li, X., Chen, S., Shi, L. and Ruoff, R.S. (2010), "Thermal transport in suspended and supported monolayer graphene grown by chemical vapor deposition", *Nano Lett.*, **10**, 1645-1651. https://doi.org/10.1021/nl9041966

Ebrahimi, F. and Barati, M.R. (2016a), "Temperature distribution effects on buckling behavior of smart heterogeneous nanosize plates based on nonlocal four-variable refined plate theory", *Int. J. Smart Nano Mater.*, **7**(3), 119-143. https://doi.org/10.1080/19475411.2016.1223203

Ebrahimi, F. and Barati, M.R. (2016b), "Vibration analysis of smart piezoelectrically actuated nanobeams subjected to magneto-electrical field in thermal environment", *J. Vib. Control*, **24**(3), 549-564. https://doi.org/10.1177/1077546316646239

Ebrahimi, F. and Barati, M.R. (2016c), "Size-dependent thermal stability analysis of graded piezomagnetic nanoplates on elastic medium subjected to various thermal environments", *Appl. Phys. A*, **122**(10), 910. https://doi.org/10.1007/s00339-016-0441-9

Ebrahimi, F. and Barati, M.R. (2016d), "Static stability analysis of smart magneto-electro-elastic heterogeneous nanoplates embedded in an elastic medium based on a four-variable refined plate theory", *Smart Mater. Struct.*, **25**(10), 105014. https://doi.org/10.1088/0964-1726/25/10/105014

Ebrahimi, F. and Barati, M.R. (2016e), "Buckling analysis of piezoelectrically actuated smart nanoscale plates subjected to magnetic field", *J. Intel. Mater. Syst. Struct.*, **28**(11), 1472-1490. https://doi.org/10.1177/1045389X16672569

Ebrahimi, F. and Barati, M.R. (2016f), "A nonlocal higher-order shear deformation beam theory for vibration analysis of size-dependent functionally graded nanobeams", *Arab. J. Sci. Eng.*, **41**(5), 1679-1690. https://doi.org/10.1007/s13369-015-1930-4

Ebrahimi, F. and Barati, M.R. (2016g), "Vibration analysis of nonlocal beams made of functionally graded material in thermal environment", *Eur. Phys. J. Plus*, **131**(8), 279. https://doi.org/10.1140/epjp/i2016-16279-y

Ebrahimi, F." and Barati, M.R. (2016h), "Dynamic modeling of a thermo–piezo-electrically actuated nanosize beam subjected to a magnetic field", *Appl. Phys. A*, **122**(4), 1-18. https://doi.org/10.1007/s00339-016-0001-3

Ebrahimi, F. and Barati, M.R. (2016i), "A unified formulation for dynamic analysis of nonlocal heterogeneous nanobeams in hygro-thermal environment", *Appl. Phys. A*, **122**(9), 792. https://doi.org/10.1007/s00339-016-0322-2

Ebrahimi, F. and Barati, M.R. (2016j), "A nonlocal higher-order refined magneto-electro-viscoelastic beam model for dynamic analysis of smart nanostructures", *Int. J. Eng. Sci.*, **107**, 183-196. https://doi.org/10.1016/j.ijengsci.2016.08.001

Ebrahimi, F. and Barati, M.R. (2016k), "Hygrothermal effects on

vibration characteristics of viscoelastic FG nanobeams based on nonlocal strain gradient theory", *Compos. Struct*., **159**, 433-444. https://doi.org/10.1016/j.compstruct.2016.09.092

Ebrahimi, F. and Barati, M.R. (2016l), "Buckling analysis of nonlocal third-order shear deformable functionally graded piezoelectric nanobeams embedded in elastic medium", *J. Brazil. Soc. Mech. Sci. Eng.*, **39**(3), 937-952. https://doi.org/10.1007/s40430-016-0551-5

Ebrahimi, F. and Barati, M.R. (2016m), "Magnetic field effects on buckling behavior of smart size-dependent graded nanoscale beams", *Eur. Phys. J. Plus*, **131**(7), 1-14. https://doi.org/10.1140/epjp/i2016-16238-8

Ebrahimi, F. and Barati, M.R. (2016n), "Buckling analysis of smart size-dependent higher order magneto-electro-thermo-elastic functionally graded nanosize beams", *J. Mech.*, 1-11. https://doi.org/10.1017/jmech.2016.46

Ebrahimi, F. and Barati, M.R. (2017), "A nonlocal strain gradient refined beam model for buckling analysis of size-dependent shear-deformable curved FG nanobeams", *Compos. Struct.*, **159**, 174-182. https://doi.org/10.1016/j.compstruct.2016.09.058

Ebrahimi, F. and Barati, M.R. (2019), "On static stability of electro-magnetically affected smart magneto-electro-elastic nanoplates", *Adv. Nano Res., Int. J.*, **7**(1), 63-75. https://doi.org/10.12989/anr.2019.7.1.063

Ebrahimi, F. and Dabbagh, A. (2016), "On flexural wave propagation responses of smart FG magneto-electro-elastic nanoplates via nonlocal strain gradient theory", *Compos. Struct*., **162**, 281-293. https://doi.org/10.1016/j.compstruct.2016.11.058

Ebrahimi, F. and Farazmandnia, N. (2017), "Thermo-mechanical vibration analysis of sandwich beams with functionally graded carbon nanotube-reinforced composite face sheets based on a higher-order shear deformation beam theory", *Mech. Adv. Mater. Struct.*, **24**, 820-829. https://doi.org/10.1080/15376494.2016.1196786

Ebrahimi, F. and Haghi, P. (2018a), "Elastic wave dispersion modelling within rotating functionally graded nanobeams in thermal environment", *Adv. Nano Res., Int. J.*, **6**(3), 201-217. https://doi.org/10.12989/anr.2018.6.3.201

Ebrahimi, F. and Haghi, P. (2018b), "A nonlocal strain gradient theory for scale-dependent wave dispersion analysis of rotating nanobeams considering physical field effects", *Coupl. Syst. Mech., Int. J.*, **7**(4), 373-393. https://doi.org/10.12989/csm.2018.7.4.373

Ebrahimi, F. and Hosseini, S.H.S. (2016a), "Thermal effects on nonlinear vibration behavior of viscoelastic nanosize plates", *J. Thermal Stresses*, **39**(5), 606-625. https://doi.org/10.1080/01495739.2016.1160684

Ebrahimi, F. and Hosseini, S.H.S. (2016b), "Double nanoplate-based NEMS under hydrostatic and electrostatic actuations", *Eur. Phys. J. Plus*, **131**(5), 1-19. https://doi.org/10.1140/epjp/i2016-16160-1

Ebrahimi, F. and Rostami, P. (2018), "Wave propagation analysis of carbon nanotube reinforced composite beams", *Eur. Phys. J. Plus*, **133**, 285. https://doi.org/10.1140/epjp/i2018-12069-y

Ebrahimi, F., Barati, M.R. and Dabbagh, A. (2016), "A nonlocal strain gradient theory for wave propagation analysis in temperature-dependent inhomogeneous nanoplates", *Int. J. Eng. Sci.*, **107**, 169-182. https://doi.org/10.1016/j.ijengsci.2016.07.008

Ebrahimi, F., Barati, M.R. and Haghi, P. (2018a), "Wave propagation analysis of size-dependent rotating inhomogeneous nanobeams based on nonlocal elasticity theory", *J. Vib. Control*, **24**, 3809-3818. https://doi.org/10.1177/1077546317711537

Ebrahimi, F., Haghi, P. and Zenkour, A.M. (2018b), "Modelling of thermally affected elastic wave propagation within rotating Mori–Tanaka-based heterogeneous nanostructures", *Microsyst. Technol.*, **24**, 2683-2693. https://doi.org/10.1007/s00542-018-3800-y

Ebrahimi, F., Dehghan, M. and Seyfi, A. (2019), "Eringen's nonlocal elasticity theory for wave propagation analysis of magneto-electro-elastic nanotubes", *Adv. Nano Res., Int. J.*, **7**(1), 1-11. https://doi.org/10.12989/anr.2019.7.1.001

Feng, C., Kitipornchai, S. and Yang, J. (2017), "Nonlinear bending of polymer nanocomposite beams reinforced with non-uniformly distributed graphene platelets (GPLs)", *Compos. Part B: Eng.*, **110**, 132-140. https://doi.org/10.1016/j.compositesb.2016.11.024

Formica, G., Lacarbonara, W. and Alessi, R. (2010), "Vibrations of carbon nanotube-reinforced composites", *J. Sound Vib.*, **329**, 1875-1889. https://doi.org/10.1016/j.jsv.2009.11.020

Gómez-Navarro, C., Burghard, M. and Kern, K. (2008), "Elastic properties of chemically derived single graphene sheets", *Nano Letters*, **8**, 2045-2049. https://doi.org/10.1021/nl801384y

Kant, T. and Babu, C. (2000), "Thermal buckling analysis of skew fibre-reinforced composite and sandwich plates using shear deformable finite element models", *Compos. Struct*., **49**, 77-85. https://doi.org/10.1016/S0263-8223(99)00127-0

Karami, B., Janghorban, M. and Tounsi, A. (2017), "Effects of triaxial magnetic field on the anisotropic nanoplates", *Steel Compos. Struct., Int. J.*, **25**(3), 361-374. https://doi.org/10.12989/scs.2017.25.3.361

Kiani, Y. (2019), "Buckling of functionally graded graphene reinforced conical shells under external pressure in thermal environment", *Compos. Part B: Eng.*, **156**, 128-137. https://doi.org/10.1016/j.compstruct.2012.11.006

Lei, Z., Liew, K. and Yu, J. (2013), "Buckling analysis of functionally graded carbon nanotube-reinforced composite plates using the element-free kp-Ritz method", *Compos. Struct.*, **98**, 160-168. https://doi.org/10.1016/j.compstruct.2012.11.006

Liew, K., Lei, Z., Yu, J. and Zhang, L. (2014), "Postbuckling of carbon nanotube-reinforced functionally graded cylindrical panels under axial compression using a meshless approach", *Comput. Methods Appl. Mech. Eng.*, **268**, 1-17. https://doi.org/10.1016/j.cma.2013.09.001

Liu, G., Chen, X. and Reddy, J. (2002), "Buckling of symmetrically laminated composite plates using the element-free Galerkin method", *Int. J. Struct. Stabil. Dyn.*, **2**, 281-294. https://doi.org/10.1142/S0219455402000634

Mehar, K., Panda, S.K., Devarajan, Y. and Choubey, G. (2019), "Numerical buckling analysis of graded CNT-reinforced composite sandwich shell structure under thermal loading", *Compos. Struct*., **216**, 406-414. https://doi.org/10.1016/j.compstruct.2019.03.002

Menasria, A., Bouhadra, A., Tounsi, A., Bousahla, A.A. and Mahmoud, S. (2017), "A new and simple HSDT for thermal stability analysis of FG sandwich plates", *Steel Compos. Struct., Int. J.*, **25**(2), 157-175. https://doi.org/10.12989/scs.2017.25.2.157

Mikoushkin, V., Shnitov, V., Nikonov, S.Y., Dideykin, A., Vul, A.Y., Sakseev, D., Vyalikh, D. and Vilkov, O.Y. (2011), "Controlling graphite oxide bandgap width by reduction in hydrogen", *Techn. Phys. Lett.*, **37**, 942. https://doi.org/10.1134/S1063785011100257

Potts, J.R., Dreyer, D.R., Bielawski, C.W. and Ruoff, R.S. (2011), "Graphene-based polymer nanocomposites", *Polymer*, **52**, 5-25. https://doi.org/10.1016/j.polymer.2010.11.042

Pradhan, S.C. and Phadikar, J.K. (2011), "Nonlocal theory for buckling of nanoplates", *Int. J. Struct. Stabil. Dyn.*, **11**(3), 411-429. https://doi.org/10.1142/S021945541100418X

Qaderi, S., Ebrahimi, F. and Seyfi, A. (2019), "An investigation of the vibration of multi-layer composite beams reinforced by graphene platelets resting on two parameter viscoelastic foundation", *SN Applied Sciences*, **1**, 399.

https://doi.org/10.1007/s42452-019-0252-7

Qiao, P., Zou, G. and Davalos, J.F. (2003), "Flexural–torsional buckling of fiber-reinforced plastic composite cantilever I-beams", *Compos. Struct.*, **60**, 205-217. https://doi.org/10.1016/S0263-8223(02)00304-5

Safarpour, H., Ghanbari, B. and Ghadiri, M. (2019), "Buckling and free vibration analysis of high speed rotating carbon nanotube reinforced cylindrical piezoelectric shell", *Appl. Math. Model.*, **65**, 428-442. https://doi.org/10.1016/j.apm.2018.08.028

Shan, L. and Qiao, P. (2005), "Flexural–torsional buckling of fiber-reinforced plastic composite open channel beams", *Compos. Struct.*, **68**, 211-224. https://doi.org/10.1016/j.compstruct.2004.03.015

Shariyat, M. (2010), "A generalized global–local high-order theory for bending and vibration analyses of sandwich plates subjected to thermo-mechanical loads", *Int. J. Mech. Sci.*, **52**, 495-514. https://doi.org/10.1016/j.ijmecsci.2009.11.010

Shen, H.-S. and Xiang, Y. (2012), "Nonlinear vibration of nanotube-reinforced composite cylindrical shells in thermal environments", *Comput. Methods Appl. Mech. Eng.*, **213**, 196-205. https://doi.org/10.1016/j.cma.2011.11.025

Shen, H.-S. and Zhang, C.-L. (2010), "Thermal buckling and postbuckling behavior of functionally graded carbon nanotube-reinforced composite plates", *Mater. Des.*, **31**, 3403-3411. https://doi.org/10.1016/j.matdes.2010.01.048

Shen, H.-S., Xiang, Y. and Lin, F. (2017a), "Nonlinear bending of functionally graded graphene-reinforced composite laminated plates resting on elastic foundations in thermal environments", *Compos. Struct.*, **170**, 80-90. https://doi.org/10.1016/j.compstruct.2017.03.001

Shen, H.-S., Xiang, Y. and Lin, F. (2017b), "Nonlinear vibration of functionally graded graphene-reinforced composite laminated plates in thermal environments", *Comput. Methods Appl. Mech. Eng.*, **319**, 175-193. https://doi.org/10.1016/j.matdes.2010.01.048

Shojaee, S., Valizadeh, N., Izadpanah, E., Bui, T. and Vu, T.-V. (2012), "Free vibration and buckling analysis of laminated composite plates using the NURBS-based isogeometric finite element method", *Compos. Struct.*, **94**, 1677-1693. https://doi.org/10.1016/j.compstruct.2012.01.012

Sobhani, A., Saeedifar, M., Najafabadi, M.A., Fotouhi, M. and Zarouchas, D. (2018), "The study of buckling and post-buckling behavior of laminated composites consisting multiple delaminations using acoustic emission", *Thin-Wall. Struct.*, **127**, 145-156. https://doi.org/10.1016/j.tws.2018.02.011

Song, M., Yang, J. and Kitipornchai, S. (2018), "Bending and buckling analyses of functionally graded polymer composite plates reinforced with graphene nanoplatelets", *Compos. Part B: Eng.*, **134**, 106-113. https://doi.org/10.1016/j.compositesb.2017.09.043

Suk, J.W., Piner, R.D., An, J. and Ruoff, R.S. (2010), "Mechanical properties of monolayer graphene oxide", *ACS Nano*, **4**, 6557-6564. https://doi.org/10.1021/nn101781v

Thai, C.H., Nguyen-Xuan, H., Nguyen-Thanh, N., Le, T.H., Nguyen-Thoi, T. and Rabczuk, T. (2012), "Static, free vibration, and buckling analysis of laminated composite Reissner–Mindlin plates using NURBS-based isogeometric approach", *Int. J. Numer. Methods Eng.*, **91**, 571-603. https://doi.org/10.1002/nme.4282

Thai, C.H., Ferreira, A., Tran, T. and Phung-Van, P. (2019), "Free vibration, buckling and bending analyses of multilayer functionally graded graphene nanoplatelets reinforced composite plates using the NURBS formulation", *Compos. Struct.*, **220**, 749-759. https://doi.org/10.1016/j.compstruct.2019.03.100

Torabi, J., Ansari, R. and Hassani, R. (2019), "Numerical study on the thermal buckling analysis of CNT-reinforced composite plates with different shapes based on the higher-order shear deformation theory", *Eur. J. Mech.-A/Solids*, **73**, 144-160. https://doi.org/10.1016/j.euromechsol.2018.07.009

Tornabene, F., Fantuzzi, N., Viola, E. and Carrera, E. (2014), "Static analysis of doubly-curved anisotropic shells and panels using CUF approach, differential geometry and differential quadrature method", *Compos. Struct.*, **107**, 675-697. https://doi.org/10.1016/j.compstruct.2013.08.038

Tounsi, A., Benguediab, S., Adda, B., Semmah, A., and Zidour, M. (2013), "Nonlocal effects on thermal buckling properties of double-walled carbon nanotubes", *Adv. Nano Res., Int. J.*, **1**(1), 1-11. https://doi.org/10.12989/anr.2013.1.1.001

Urthaler, Y. and Reddy, J. (2008), "A mixed finite element for the nonlinear bending analysis of laminated composite plates based on FSDT", *Mech. Adv. Mater. Struct.*, **15**, 335-354. https://doi.org/10.1080/15376490802045671

Van Es, M. (2001), "Polymer-clay nanocomposites", Ph.D. Thesis; Delft University, Delft, Netherlands.

Wang, Z.-X. and Shen, H.-S. (2011), "Nonlinear vibration of nanotube-reinforced composite plates in thermal environments", *Computat. Mater. Sci.*, **50**, 2319-2330. https://doi.org/10.1016/j.commatsci.2011.03.005

Wang, Q., Shi, D., Liang, Q. and Pang, F. (2017), "Free vibrations of composite laminated doubly-curved shells and panels of revolution with general elastic restraints", *Appl. Math. Model.*, **46**, 227-262. https://doi.org/10.1016/j.apm.2017.01.070

Wattanasakulpong, N. and Ungbhakorn, V. (2013), "Analytical solutions for bending, buckling and vibration responses of carbon nanotube-reinforced composite beams resting on elastic foundation", *Computat. Mater. Sci.*, **71**, 201-208. https://doi.org/10.1016/j.commatsci.2013.01.028

Wu, H., Yang, J. and Kitipornchai, S. (2016), "Nonlinear vibration of functionally graded carbon nanotube-reinforced composite beams with geometric imperfections", *Compos. Part B: Eng.*, **90**, 86-96. https://doi.org/10.1016/j.compositesb.2015.12.007

Yang, J., Wu, H. and Kitipornchai, S. (2017), "Buckling and postbuckling of functionally graded multilayer graphene platelet-reinforced composite beams", *Compos. Struct.*, **161**, 111-118. https://doi.org/10.1016/j.compstruct.2016.11.048

Yas, M. and Samadi, N. (2012), "Free vibrations and buckling analysis of carbon nanotube-reinforced composite Timoshenko beams on elastic foundation", *Int. J. Press. Vessels Pip.*, **98**, 119-128. https://doi.org/10.1016/j.ijpvp.2012.07.012

Yazid, M., Heireche, H., Tounsi, A., Bousahla, A.A. and Houari, M.S.A. (2018), "A novel nonlocal refined plate theory for stability response of orthotropic single-layer graphene sheet resting on elastic medium", *Smart Struct. Syst., Int. J.*, **21**(1), 15-25. https://doi.org/10.12989/sss.2018.21.1.015

Zhang, L., Lei, Z. and Liew, K. (2015), "Vibration characteristic of moderately thick functionally graded carbon nanotube reinforced composite skew plates", *Compos. Struct.*, **122**, 172-183. https://doi.org/10.1016/j.ijpvp.2012.07.012

Zhang, Z., Li, Y., Wu, H., Zhang, H., Wu, H., Jiang, S. and Chai, G. (2018), "Mechanical analysis of functionally graded graphene oxide-reinforced composite beams based on the first-order shear deformation theory", *Mech. Adv. Mater. Struct.*, 1-9. https://doi.org/10.1080/15376494.2018.1444216

Zhao, Z., Feng, C., Wang, Y. and Yang, J. (2017), "Bending and vibration analysis of functionally graded trapezoidal nanocomposite plates reinforced with graphene nanoplatelets (GPLs)", *Compos. Struct.*, **180**, 799-808. https://doi.org/10.1016/j.compstruct.2017.08.044

Zhen, W. and Wanji, C. (2006), "Free vibration of laminated composite and sandwich plates using global–local higher-order theory", *J. Sound Vib.*, **298**, 333-349. https://doi.org/10.1016/j.jsv.2006.05.022

Zhu, P., Lei, Z. and Liew, K.M. (2012), "Static and free vibration analyses of carbon nanotube-reinforced composite plates using finite element method with first order shear deformation plate theory", *Compos. Struct.*, **94**, 1450-1460. https://doi.org/10.1016/j.compstruct.2011.11.010

CC